AD

16

TECHNICAL REPORT ECOM-02253-F

AD662070

STUDY OF HIGH POWER ELECTROSTATICALLY FOCUSED KLYSTRONS

FINAL REPORT

by

T. H. Luchsinger and W. R. Day

November 196,

Sponsored by:
Advanced Research Projects Agency
Project Defender, ARPA Order No. 436

ECOM

UNITED STATES ARMY ELECTRONICS COMMAND · FORT MONMOUTH, N.J.

Contract No. DA 28-043 AMC-02253(E)

LITTON INDUSTRIES
ELECTRON TUBE DIVISION
960 INDUSTRIAL ROAD · SAN CARLOS, CALIFORNIA

86

Reports Control Symbol
RCS-OSD-1366

NOTICES

DISCLAIMERS

The findings in this report are not to be construed as an official Department of the Army position, unles so designated by other authorized documents.

The citation of trade names and names of manufacturers in this report is not to be construed as official Government indorsement or approval of commercial products or services referenced herein.

DISPOSITION

Destroy this report when it is no longer needed. Do not return it to the originator.

Technical Report ECOM-02253-F November 1967

STUDY OF HIGH-POWER ELECTROSTATICALLY FOCUSED KLYSTRONS

FINAL REPORT

1 May 1966 to 28 August 1967

Contract No. DA 28-043-AMC-02253(E)
Project No. 7910.21.223.04.00

Prepared by
T. H. Luchsinger and W. R. Day

Research Department
Litton Industries
Electron Tube Division
San Carlos, California

For
U. S. Army Electronics Command, Fort Monmouth, N.J., 07703
Sponsored by
Advanced Research Projects Agency, ARPA Order No. 436

TABLE OF CONTENTS

LIST OF ILLUSTRATIONS

LIST OF ILLUSTRATIONS (Cont.)

PURPOSE

The purpose of this program was to study the feasibility of developing a high power, broadband, C-band electrostatically focused klystron (ESFK) suitable for use in phased array systems.

Specifically, this program investigated the feasibility of employing higher perveance beams in ESFK's. A higher beam perveance results in better gain times bandwidth and efficiency times bandwidth characteristics and in lower beam voltages for a given beam power level.

Even though the ultimate application for this device was in C-band, the experimental work of this program was done in S-band to utilize existing designs and test equipment. The experimental results, however, were evaluated with the view of determining the operating limits of C-band ESFK's.

The electrical design objectives were as follows:

Frequency	S-band
Peak rf power output (nom)	250 kW
Cathode voltage	40 kV (max)
Modulating anode voltage	Variable between 30 and 56 kV
Beam perveance	Variable between 1.0×10^{-6} to 2.5×10^{-6} $A/V^{3/2}$
Gun perveance	1.5×10^{-6} $A/V^{3/2}$

The work under this contract was made possible by the support of the Advanced Research Projects Agency under Order No. 436, under the technical guidance of the United States Army Electronics Command.

ABSTRACT

This report covers a 15-month program of experimental study to establish the feasibility of employing higher perveance beams in ESFK's, which together with other broadband techniques (filter, extended interaction cavity) would lead to ten percent bandwidth. In order to keep the tube design as simple as possible, this program was undertaken only to study the feasibility of employing higher beam perveances in ESFK's.

In addition to the experimental study, further theoretical studies were made on a triple gap extended interaction cavity leading to a 1 MW peak power C-band klystron with ten percent bandwidth. Studies of beam power and perveance limits for ESFK's were made. An improved method was developed for calculating small-signal gain of ESFK's which accounts for the effect of the electrostatic field of the lens on the electron bunching process.

During this program, one beam tester and one electrostatically focused klystron were built. By utilizing very low perveances ($.8 \times 10^{-6}$ $A/V^{3/2}$) efficiencies of up to 43 percent were achieved. By increasing the perveance to 1.5×10^{-6} $A/V^{3/2}$ the efficiency dropped to 36 percent. Beam perveances higher than approximately 1.75×10^{-6} $A/V^{3/2}$ do not appear useful in ESFK's.

GLOSSARY

A	Arbitrary constant
a	Drift tube radius
B	Arbitrary constant
b	Beam radius
b_{ave}	Average beam radius
d	Gap length
f	Frequency
G_o	Beam conductance
$g_{n,n-1}$	Transconductance between cavity n and n-1
H	Height of resonator
I_o	dc beam current
i_o	dc current density
i_1	ac current density
i	Convection current density
$\hat{i}$	ac current
$\hat{i}_1$	ac current at entrance plane
$\hat{i}_2$	ac current at exit plane
K,k	Beam perveance
L,ℓ	Drift distance (lens period)
M	Gap coupling coefficient
N	dc beam power
Q	Resonator quality factor
R_{sh}	Resonator shunt resistance

GLOSSARY (Cont.)

r_o	Beam radius
S	Lens gap width
T	Thickness of lens electrode
t	Time
$\hat{V}, \hat{v}$	ac velocity
V_o	dc beam voltage
V_m	Voltage at potential minimum
$\hat{V}_1$	ac velocity at entrance plane
$\hat{V}_2$	ac velocity at exit plane
W_o	dc beam power
w	Resonator wall thickness
Z_b	Beam impedance
Z_o	$\mu_m^{3/2}/\omega\epsilon\sqrt{K}$
z_m	Position of potential minimum
z	Distance variable
γ	Propagation constant
Δf	Bandwidth
ϵ	Dielectric constant of free space
η	Electron charge-to-mass ratio
λ	Wavelength
ρ	Space charge density
ρ_o	dc charge density
ρ_1	ac charge density

GLOSSARY (Cont.)

μ	Velocity variable
μ_o	dc beam velocity
μ_1	dc velocity at entrance plane
ϕ_m	Normalized value of minimum potential
ω	Angular frequency
ω_q	Reduced plasma frequency

1.0 FACTUAL DATA

1.1 INTRODUCTION

This program was a continuation of the study of high power electrostatically focused klystrons, where 1 MW peak power was successfully demonstrated. The primary goal of this new program was to investigate the feasibility of employing higher perveance beams in ESFK's. Until then only beam perveances of up to 1.0×10^{-6} $A/V^{3/2}$ had been successfully employed in ESFK's. Since this new type of tube does not require any external magnetic focusing structures and since all the electrostatic focusing fields are entirely enclosed within the metal envelope of the tube, it is feasible to operate tubes in close proximity to each other. This suggests that it may be practical to stack a large number of ESFK's together in a matrix with center-to-center spacings commensurate with that required for phased array radar systems.

The specific electrical performance objectives for the tube (L-5114) were as follows:

Frequency	3000 MHz (Nom)
Peak rf power output	Variable between 130 and 320 kW
Cathode voltage	40 kV
Gun perveance	1.5×10^{-6} $A/V^{3/2}$
Beam perveance	Variable between 1.0×10^{-6} and 2.5×10^{-6} $A/V^{3/2}$
Modulating anode voltage	Variable between 30 and 56 kV
Beam current	Variable between 8 and 20 Amps
RF pulse length	10 μsec
Duty	.001
Gain	36 dB

This report will first discuss the general design approach to the objectives of this program, then specific areas such as the design of the focusing system, the mechanical design of the tube, the beam tester, the test results and further studies of important design consideration for ESFK's will be discussed in detail.

1.2 TECHNICAL DISCUSSION

The broadbanding of klystron amplifiers has received considerable attention. Because the basic operating principle of a klystron depends on the use of resonant structures, there are inherent bandwidth limitations on any klystron design.

The bandwidth of a klystron amplifier is essentially determined by the R_{sh}/Q of the output circuit with the beam impedance Z_b:

$$\frac{\Delta f}{f} \propto \frac{R_{sh}}{Q} \times \frac{1}{Z_b}$$

The beam impedance Z_b is related to the beam perveance K and the beam power N through the following relation:

$$Z_b = \frac{V_o}{I_o} = \frac{1}{N^{1/5} K^{4/5}}$$

As one can see from this equation, the beam impedance is a strongly varying function of the beam perveance, but varies much less as a function of the beam power.

Increasing the beam perveance is therefore a crucial design consideration for broadbanding klystrons. A higher beam perveance also has the added advantage of reducing the required beam voltage for a given beam power level. A lower beam voltage is, of course, also attractive for an ESFK amplifier, because it reduces the voltage holdoff gradient in the focusing lens housing. A lower beam voltage is also desirable from other considerations, such as lower X-ray level, reduced voltage gradients in the gun and gun insulator, and lower insulation requirements in the power supply. The beam voltage, V_o, the beam power and the beam perveance are related by:

$$V_o = \left(\frac{N}{K}\right)^{2/5}$$

Limitations on the beam perveance are imposed both by the gun design and the focusing system. In conventional magnetically focused klystrons, beam perveance values of up to 3×10^{-6} $A/V^{3/2}$ have been successfully used with solid beams.

The highest beam perveance which had been successfully used up to that time with electrostatic focusing was 1×10^{-6} $A/V^{3/2}$. This program was therefore primarily concerned with an evaluation of the feasibility of using higher beam perveance values in ESFK amplifiers.

1.3 GENERAL DESIGN CONSIDERATIONS

A schematic layout of the tube is shown in Fig. 1. The test vehicle was a modified version of an existing ESFK, the L-3668H. The main difference was the addition of a modulating anode, so that the beam perveance could be changed over

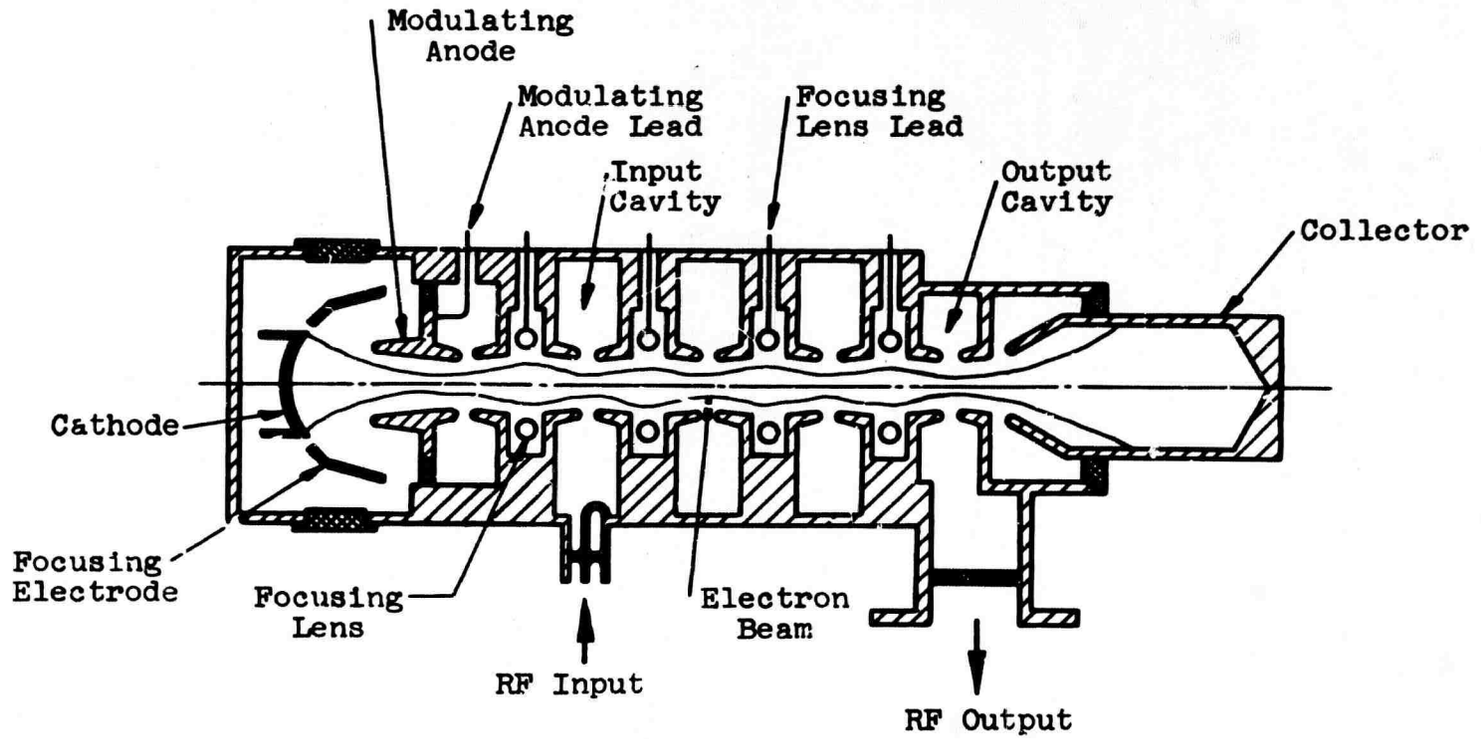

SCHEMATIC LAYOUT OF THE TUBE

Fig. 1

a wide range. The design of the experimental tube was optimized at a beam perveance of 1.5×10^{-6} $A/V^{3/2}$. The gun perveance was also 1.5×10^{-6} $A/V^{3/2}$. Therefore, for a beam perveance of 1.5×10^{-6} $A/V^{3/2}$ the modulating anode was operated at body potential. The nominal beam voltage was 40 kV and the beam current for a 1.5×10^{-6} perveance was 12 amps.

1.4 ELECTRICAL DESIGN

1.4.1 Gun Design

A modified Pierce gun, consisting of a cathode, focus electrode and modulating anode was designed for this tube. This electron gun was designed with the following characteristics:

Perveance	1.5×10^{-6} $A/V^{3/2}$
Modulating anode voltage	Variable from 30.5 to 56 kV, 40 kV design center
Cathode current	Variable between 8 and 20 Amps, 12 Amp design center
Beam power	Variable between 320 and 800 kW
Cathode diameter	1.97 cm
Cathode area	3.19 cm^2
Cathode half-angle	25°
Beam diameter at min. and 40 kV	.9 cm
Convergence ratio area	5.0

The electron gun was designed by using a precision resistance network analogue in conjunction with a high speed digital computer. Since this gun had to operate at different

mcd-anode voltages, it was important that the location and diameter of the beam minimum did not change much as a function of mod-anode voltage. Trajectories were calculated for mod-anode voltages of 40, 50 and 56 kV, which corresponds to beam perveances of 1.5×10^{-6}, 2.1×10^{-6} and 2.5×10^{-6} $A/V^{3/2}$. Figure 2 shows the electron trajectories for a gun, with the mod-anode operating at 40 kV. The beam diameter at the minimum position is .355". By increasing the mod-anode voltage to 50 kV, and to 56 kV, the beam diameter changed slightly to .368" and .384", respectively.

1.4.2 Focusing Structure

Four negative Einzel lens systems were used in this tube, with the first lens system located adjacent to and upstream from the input cavity. The other three lens systems were located between cavities.

The primary problem was to develop a lens system which focused beams of variable perveances (from 1.0 to 2.5×10^{-6} $A/V^{3/2}$) over a fixed lens period with a minimum of spherical aberration. The design of the focusing system was carried out by means of a resistance network analogue in combination with a high speed digital computer. In Fig. 3 the trajectories for perveances between 1.5×10^{-6} and 2.5×10^{-6} $A/V^{3/2}$ are shown. This Figure indicates the system might not be stable at a perveance of 2.5×10^{-6} $A/V^{3/2}$, because the electrons do not come back to their original diameter.

At the design center for a beam perveance of 1.5×10^{-6} $A/V^{3/2}$, the significant design parameters for these lenses were:

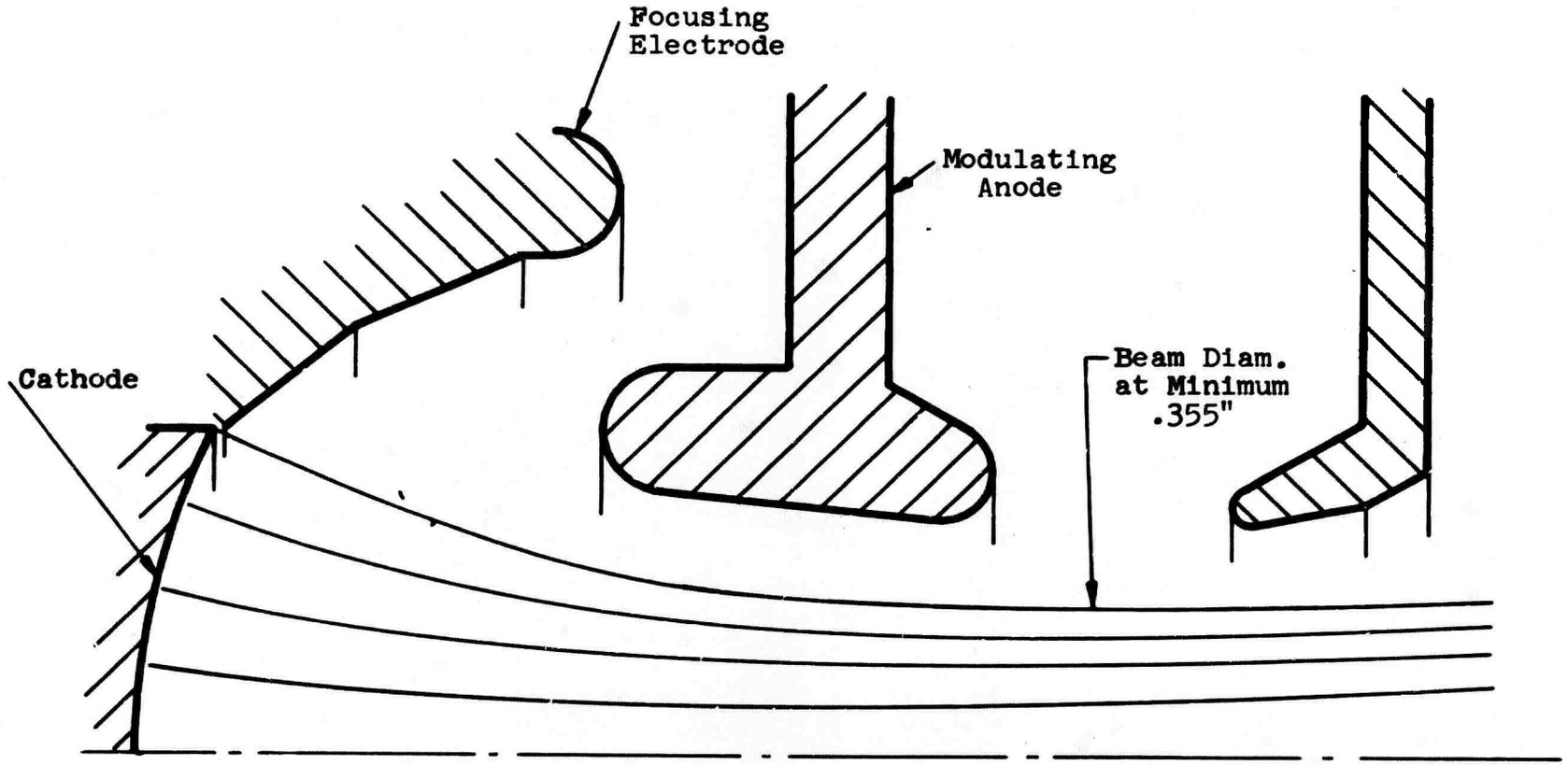

ELECTRON TRAJECTORIES AT A CATHODE VOLTAGE OF 40 KV (BEAM PERVEANCE IS 1.5×10^{-6} $A/V^{3/2}$)

Fig. 2

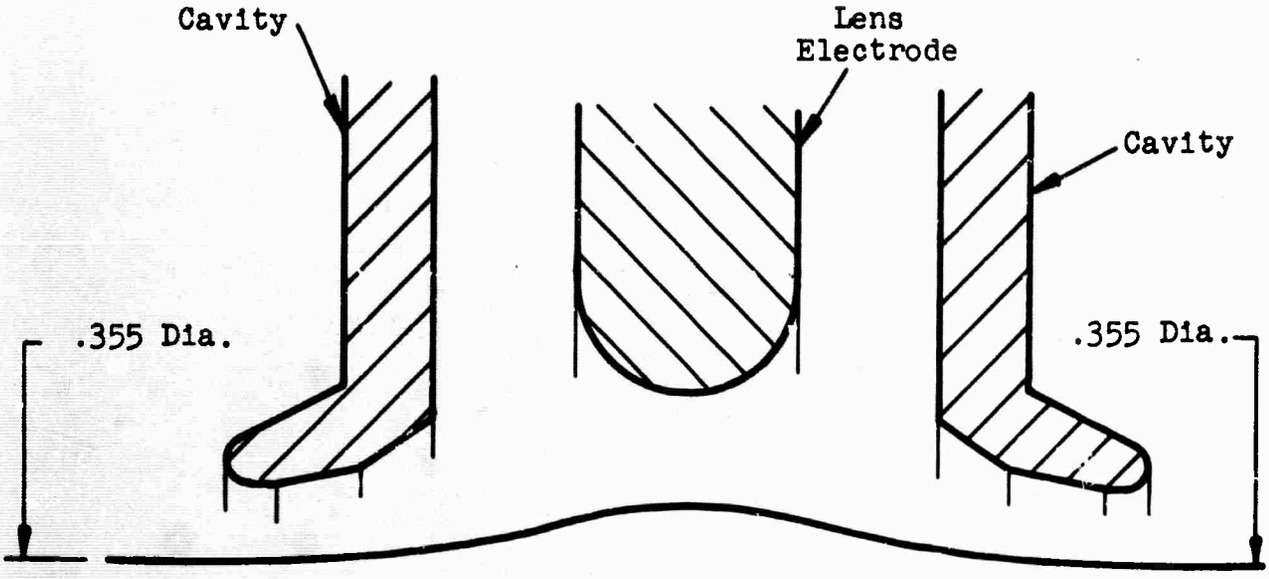

$k = 1.5 \times 10^{-6} A/V^{3/2}$

$k = 2.1 \times 10^{-6} A/V^{3/2}$

$k = 2.5 \times 10^{-6} A/V^{3/2}$

ELECTRON TRAJECTORIES FOR A 1.5, 2.1, and $2.5 \times 10^{-6} A/V^{3/2}$ PERVEANCE LENS SYSTEM

Fig. 3

Focusing period, p	3.25 cm
Minimum beam diameter, $2b_{min}$	.9 cm
Maximum beam diameter, $2b_{max}$	1.15 cm
I.D. of interaction gap, 2a	1.395 cm
I.D. of lens electrode	1.92 cm
Ratio $\frac{a}{b_{min}}$	1.55
Propagation constant γ	1.59×10^{-2}
Gap length, d	.7 cm
Normalized drift tube radius, γa	1.11
Normalized gap length, γd	1.11

1.5 TUBE CONSTRUCTION AND PROCESSING

The tube was constructed from the following major subassemblies:

a. Main body (Fig. 4)

b. Gun with gun ceramic (Fig. 5)

c. Collector with collector ceramic (Fig. 6)

d. RF output window (Fig. 7)

e. Exhaust tubulation with 1 ℓ/sec vacion pump.

The main body of the tube consists of the modulating anode, three buncher cavity assemblies with capacitive tuner and lens system, and the output cavity with an inductive tuner. To reduce instabilities, the first two buncher cavities were partially iron-plated. The measured Q_o of these cavities was 1600 compared with the all-copper penultimate cavity Q_o of 3200. The unloaded Q of the output cavity was 4000, the loaded Q was 45; therefore the circuit efficiency was 98.9%.

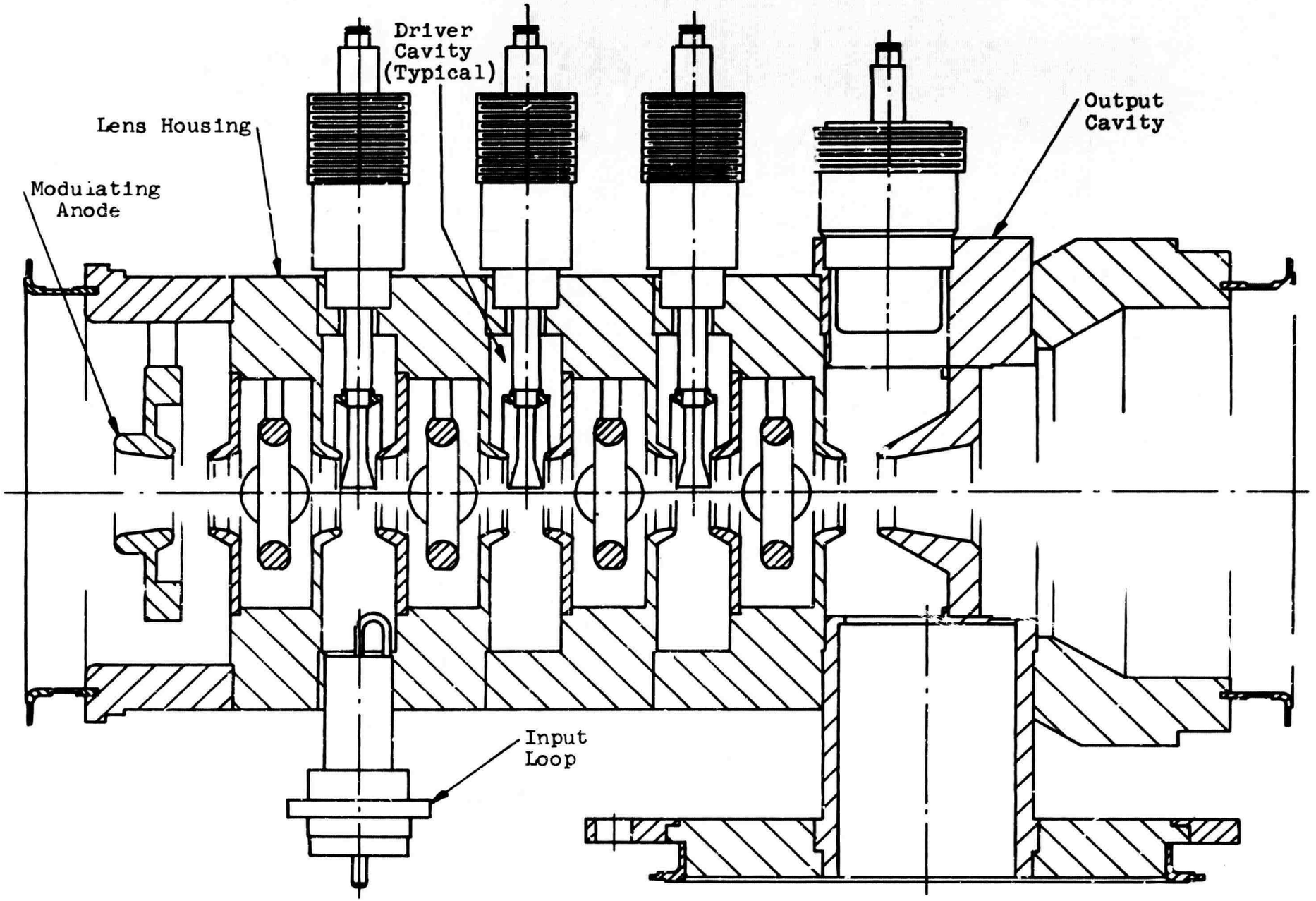

MAIN BODY ASSEMBLY L-5114
Fig. 4

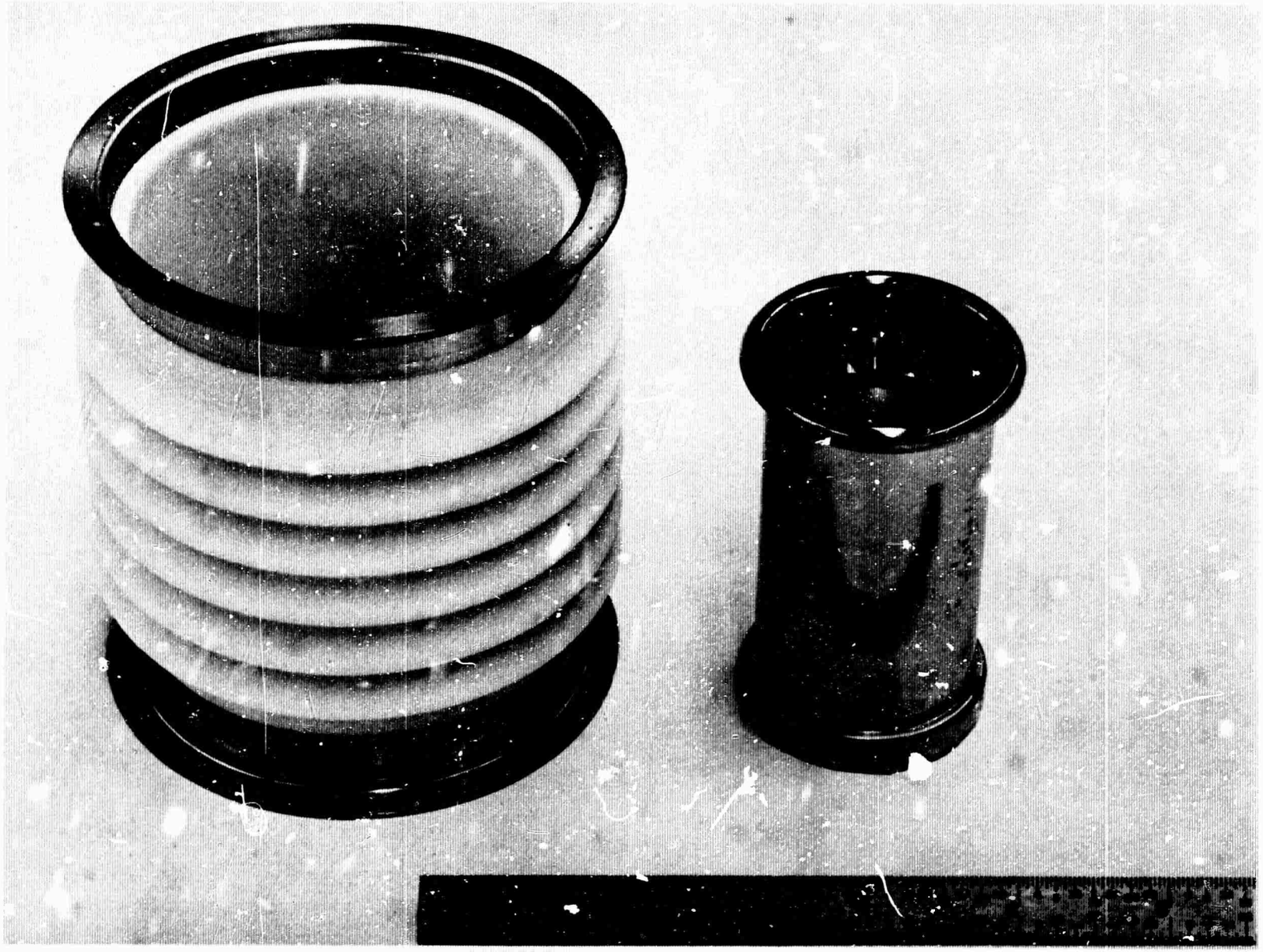

GUN WITH GUN CERAMIC
L-5114

Fig. 5

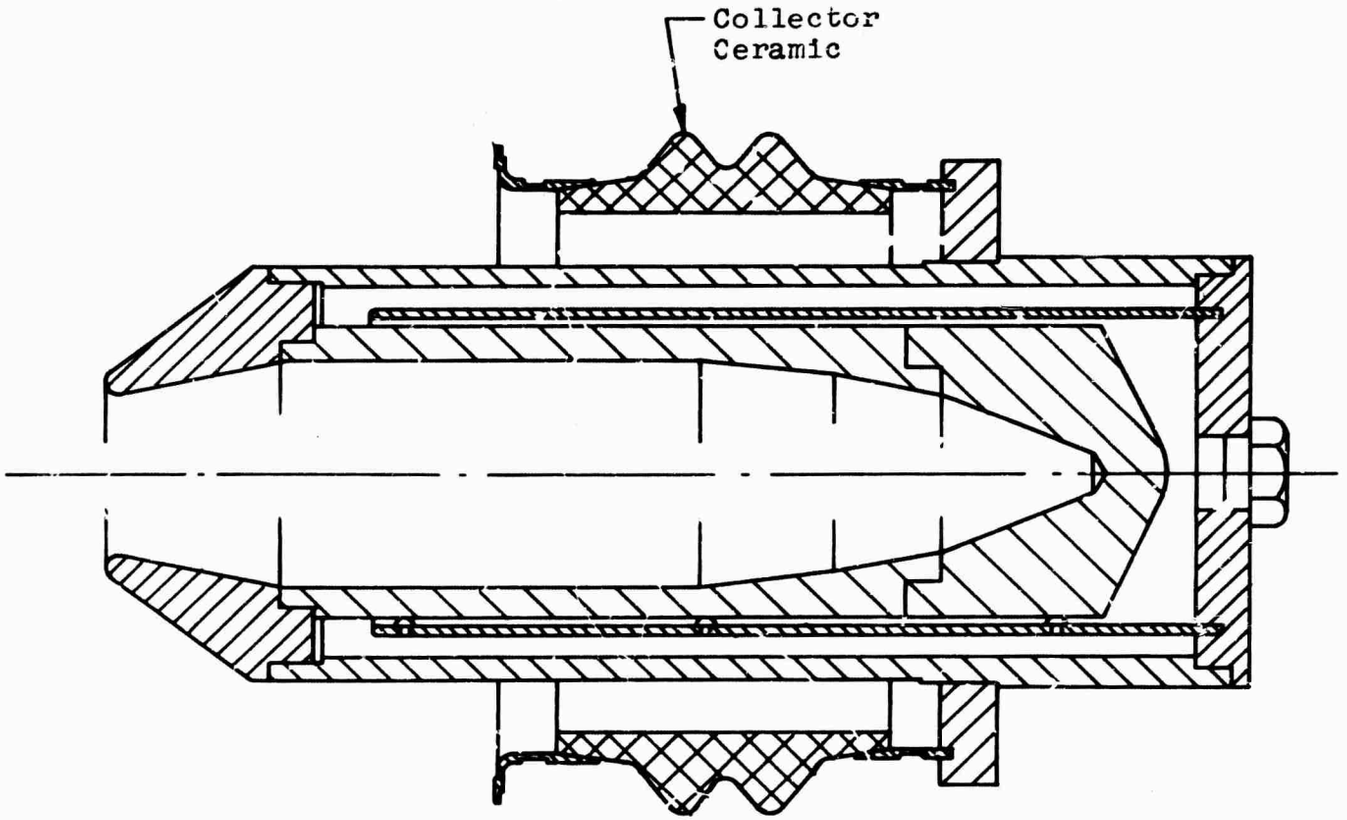

COLLECTOR WITH COLLECTOR CERAMIC
L-5114

Fig. 6

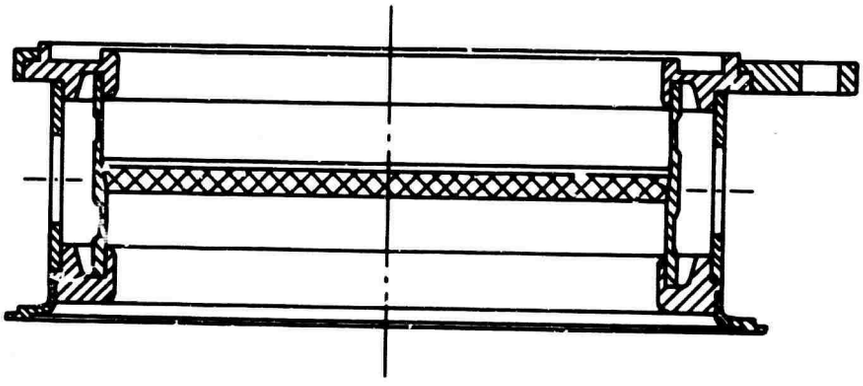

RF OUTPUT WINDOW
L-5114

Fig. 7

The rf output window and collector, with slight modification for the new beam profile, were taken over from the L-3975, a 1 MW peak power tube.

The ceramic chosen for the gun envelope provided a minimum 3-inch air gap between the high voltage header flange and ground. The cathode emission coating was a standard barium-strontium carbonate mixture, cataphoretically deposited onto an electronic grade 220 nickel base. The gun, collector, rf output window and exhaust tubulation were attached to the tube by means of weld flanges.

The tube was exhausted with standard Litton exhaust procedures which included bakeout at 625°C.

1.6 EXPERIMENTAL RESULTS

Figure 8 shows the tube (L-5114) ready for test. During testing each lens was tied to a separate dc power supply, which allowed greater flexibility in optimizing the beam focusing. An E-H tuner was used between the tube output circuit and load in order to match the output coupling over the entire operating levels.

First of all, dc transmission tests were made at different voltages and perveances. As can be seen in Fig. 9, the dc beam transmission dropped badly between voltages of about 30 and 35 kV and at perveances higher than 1.3×10^{-6} $A/V^{3/2}$. This indicated that something in the focusing system did not work as anticipated. The space charge limited perveance was measured to be 1.73×10^{-6} $A/V^{3/2}$, which was considerably higher than the design perveance of 1.5×10^{-6} $A/V^{3/2}$. All important dimensions, which could have influenced the perveance value, were checked and it was found that the cathode head was .020" too close to the modulating anode. To be sure

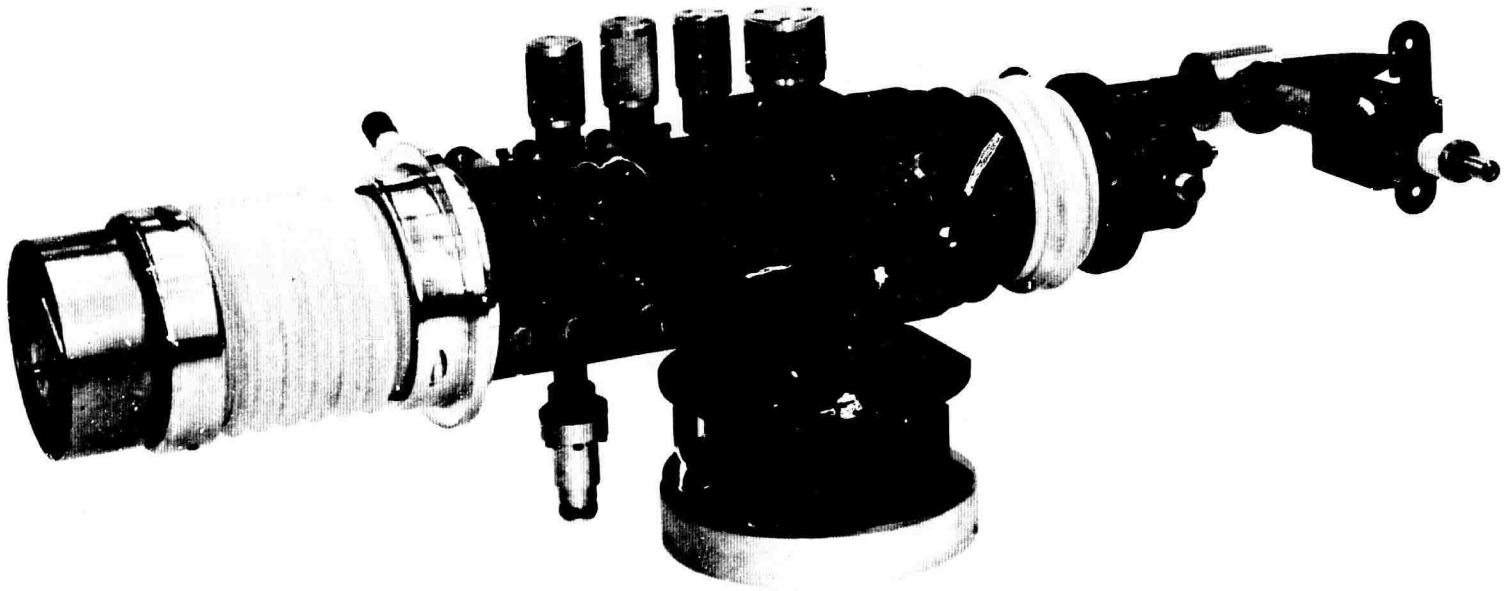

PHOTOGRAPH OF THE L-5114 ELECTROSTATICALLY FOCUSED KLYSTRON READY FOR TEST

Fig. 8

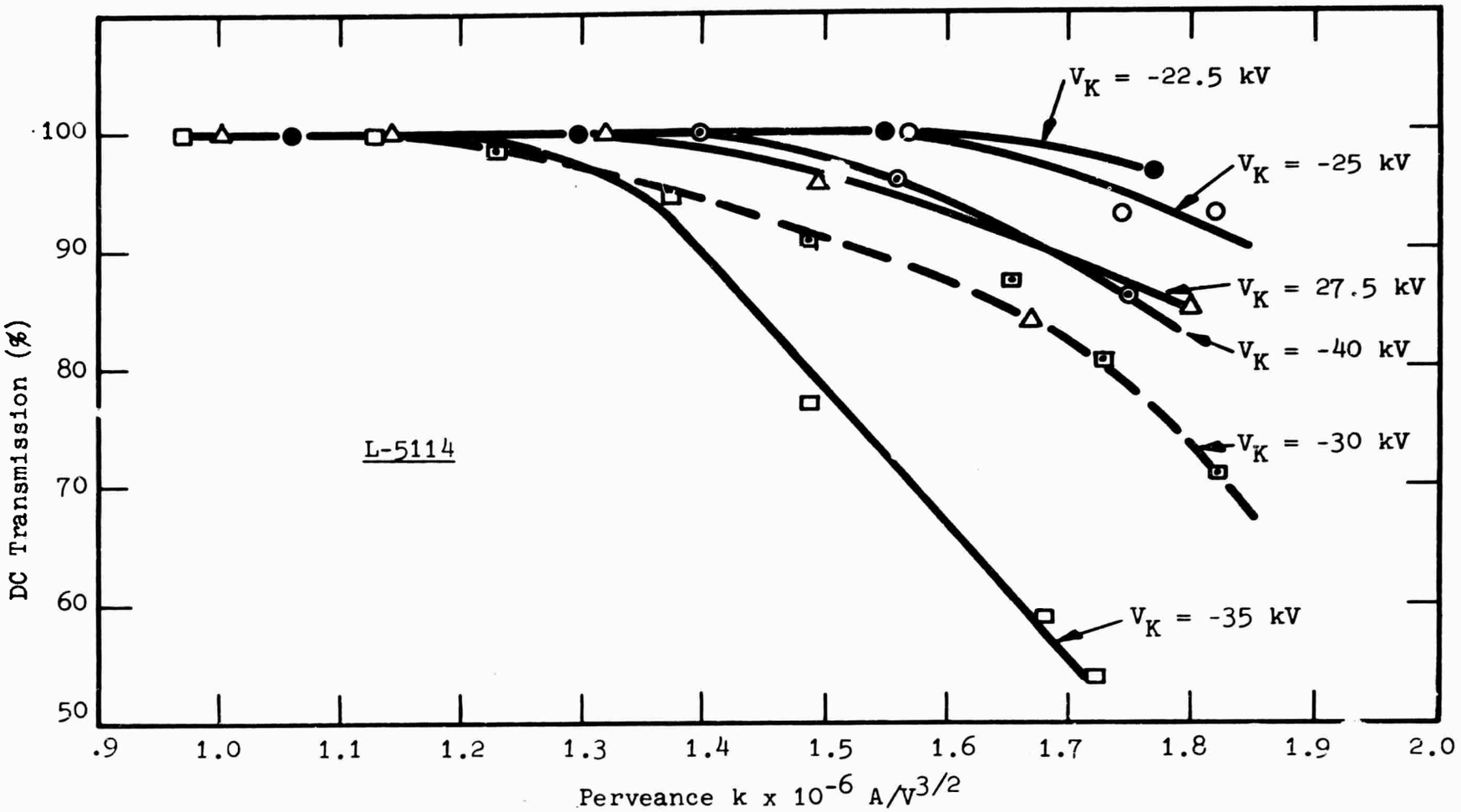

DC TRANSMISSION VERSUS PERVEANCE FOR DIFFERENT CATHODE VOLTAGES

Fig. 9

that this was the only error, a check run with the gun dimension actually used in the tube was made on the resistor network analogue and digital computer. The result was a perveance of 1.74×10^{-6} $A/V^{3/2}$, which was very close to the measured value of 1.73×10^{-6} $A/V^{3/2}$. The beam diameter at the minimum position was now .400", which was .040" greater at that particular perveance than the diameter used for designing the focusing lens system. It was concluded that this may have been the reason for the poor dc beam transmission. Nevertheless, before making further decisions, it was found worthwhile to make rf tests with the tube.

RF output power as a function of rf drive power is shown in Fig. 10. The beam voltage was 25 kV and everything, including lens voltages, cavity tuners and E-H tuner, was optimized for each drive level. For the second curve, the tuning was held fixed and it shows a typical klystron drive characteristic. The tube was operated at 25 kV.

In the next curves, Figs. 11 and 12, rf output power versus cathode voltage is shown. The perveance was 1.2×10^{-6} and 1.73×10^{-6} $A/V^{3/2}$, respectively. At higher voltages, it was impossible to get useful results at higher perveances.

In Figs. 13 and 14, the efficiency and rf output power versus perveance for cathode voltages of 25 and 42 kV are shown. These data clearly demonstrate that the efficiency is dropping off as the perveance is increased. Figure 15 shows efficiency versus cathode voltage for different perveance values. The degradation of efficiency with increasing beam perveance can be largely attributed to the poor

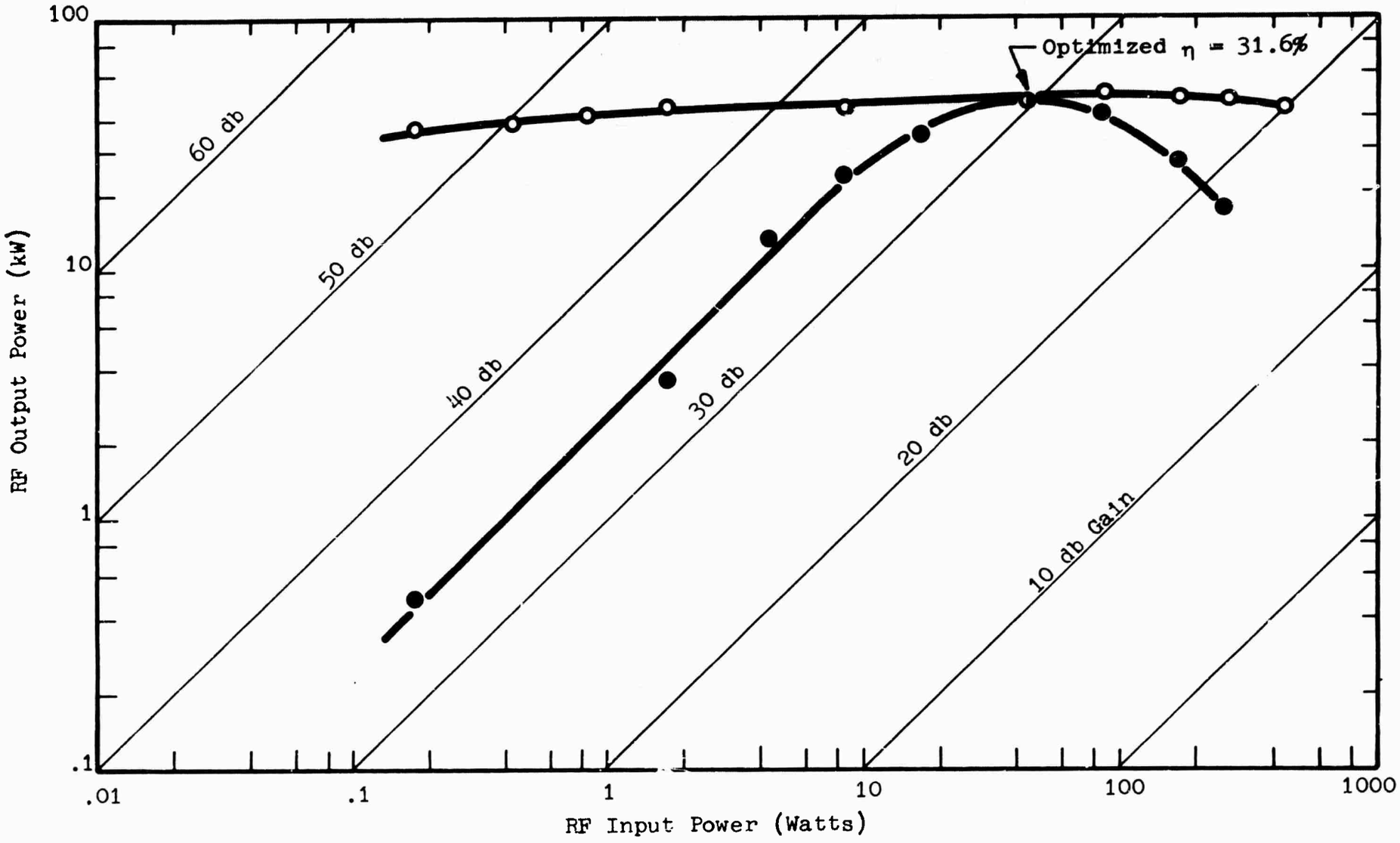

RF OUTPUT POWER VS DRIVE POWER, L-5114 NO. 1
V_k = -25 kV, f = 3040 MHz, k = 1.52 x 10^{-6} $A/V^{3/2}$

Fig. 10

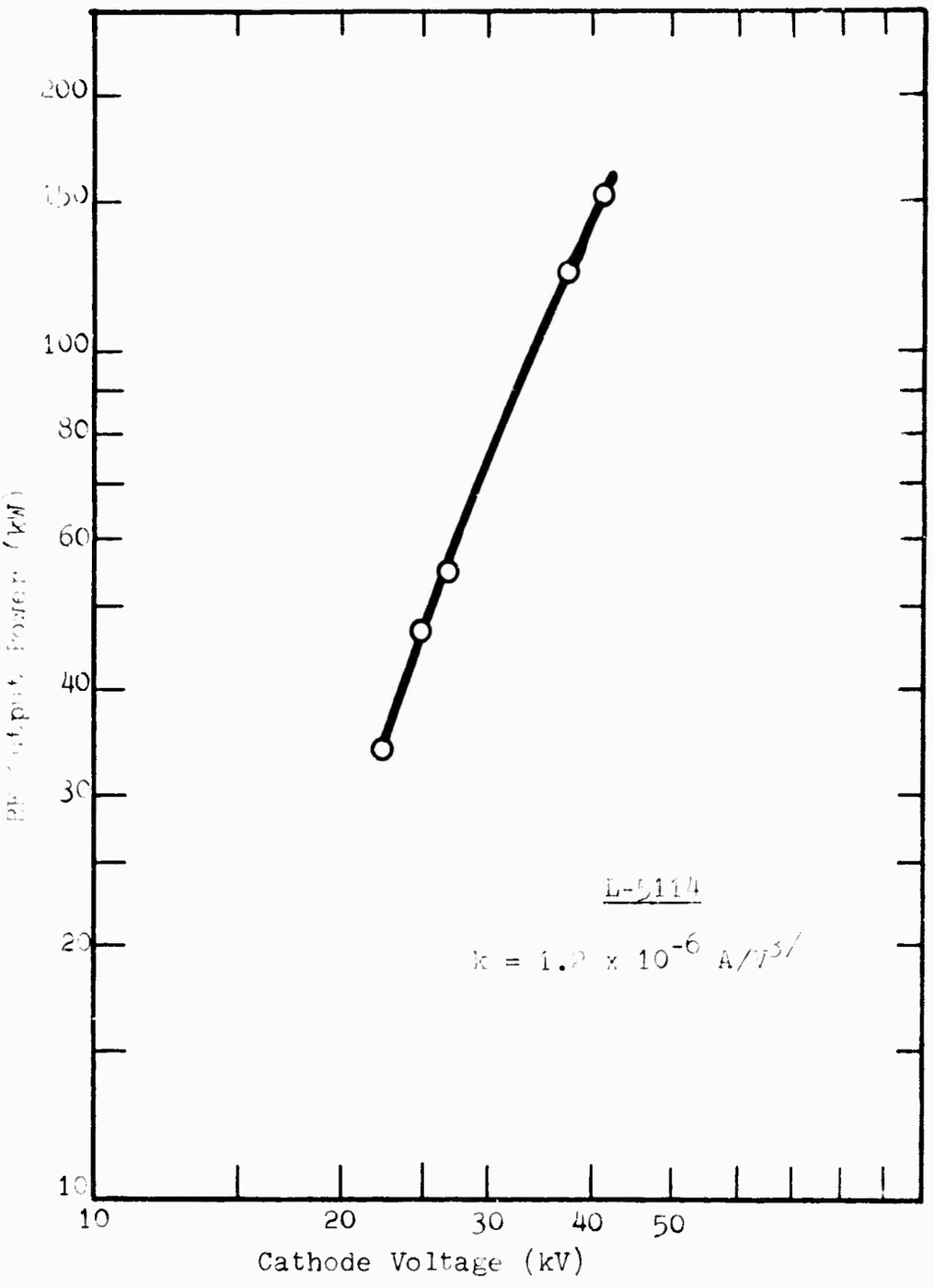

RF OUTPUT POWER VERSUS CATHODE VOLTAGE

$k = 1.2 \times 10^{-6}\ A/V^{3/2}$

Fig. 11

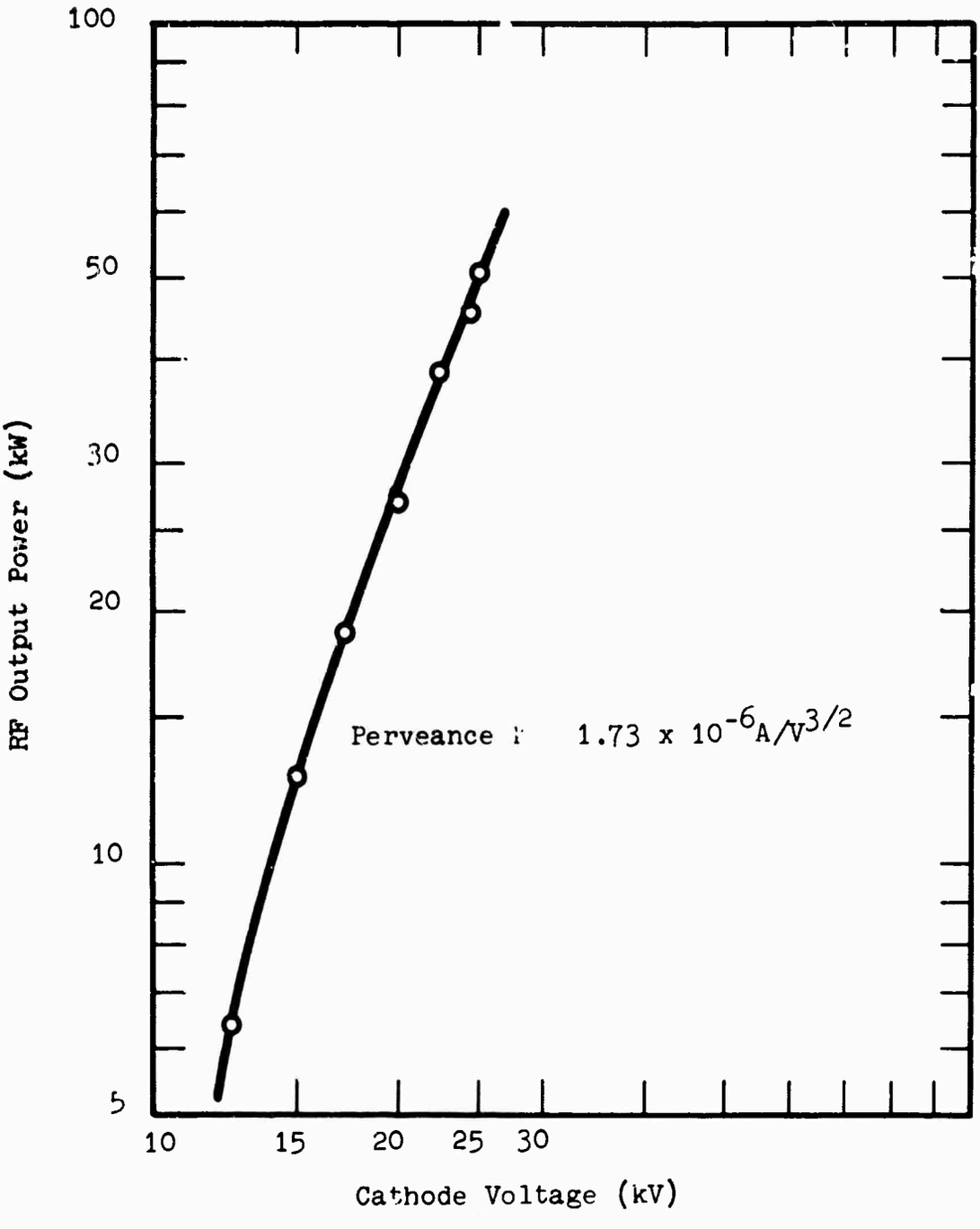

RF OUTPUT POWER VS CATHODE VOLTAGE
L-5114 NO. 1

Fig. 12

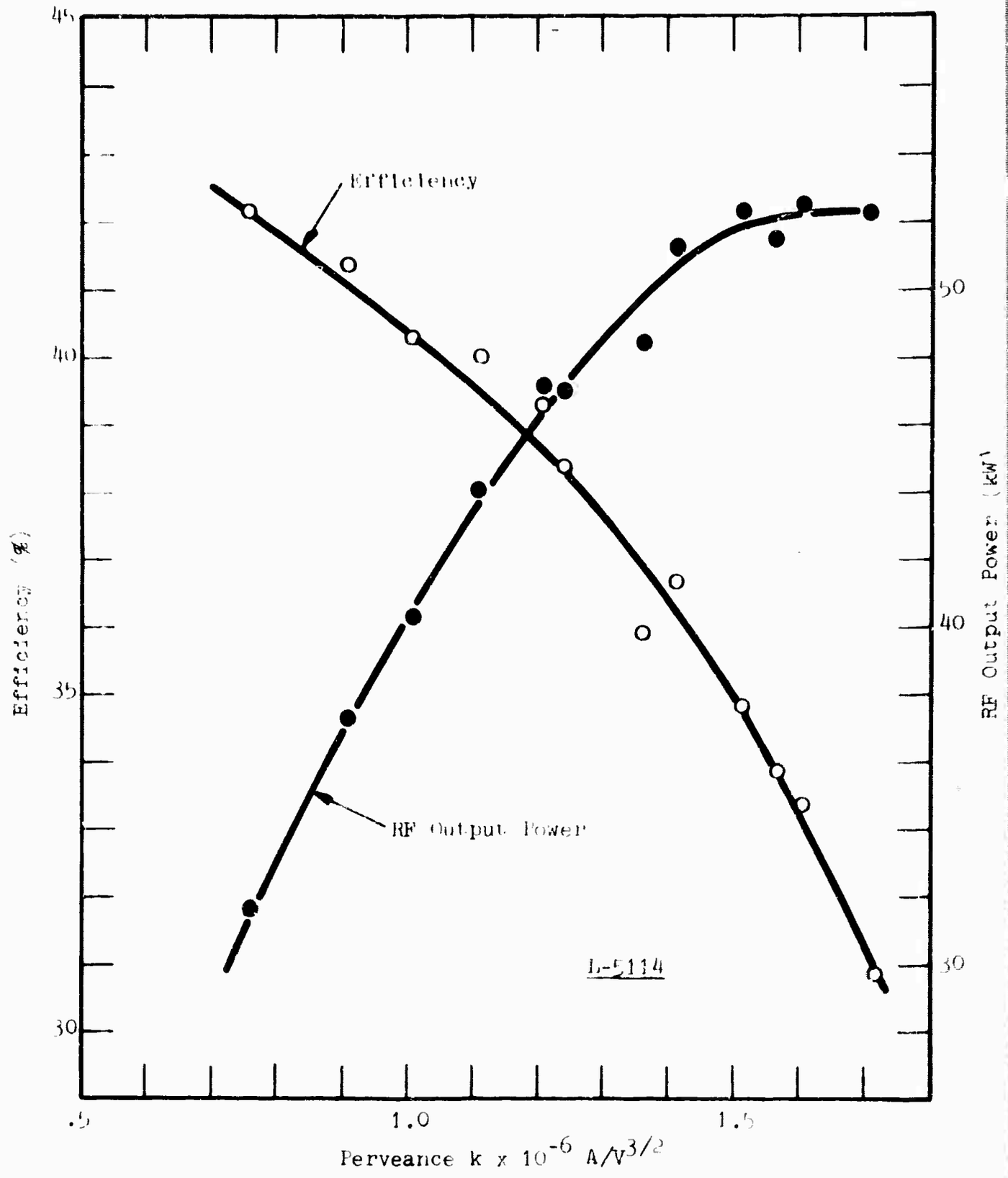

EFFICIENCY AND RF OUTPUT POWER VERSUS PERVEANCE

V_K = -25 kV

Fig. 13

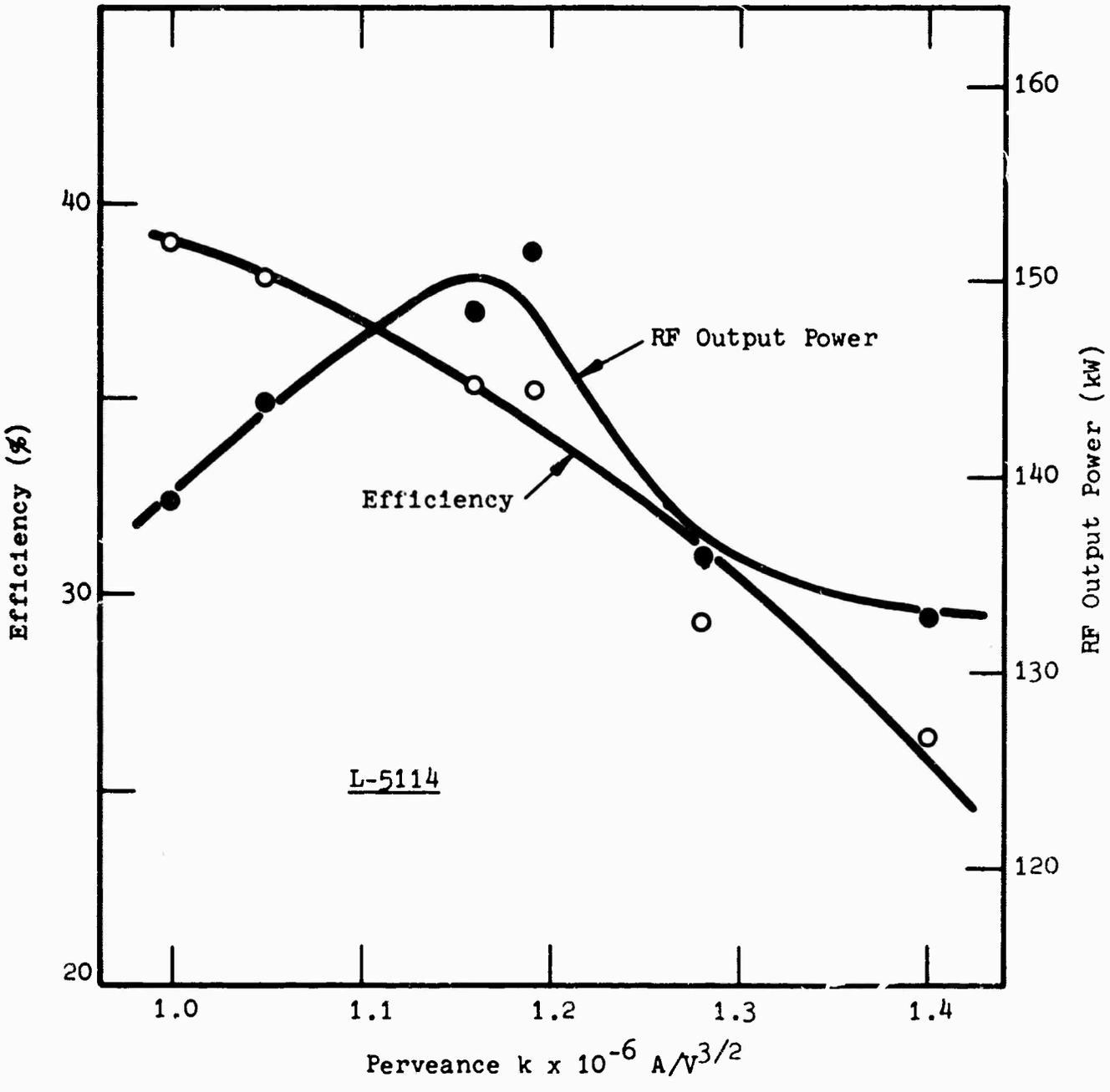

EFFICIENCY AND RF OUTPUT POWER VERSUS PERVEANCE

V_K = -42 kV

Fig. 14

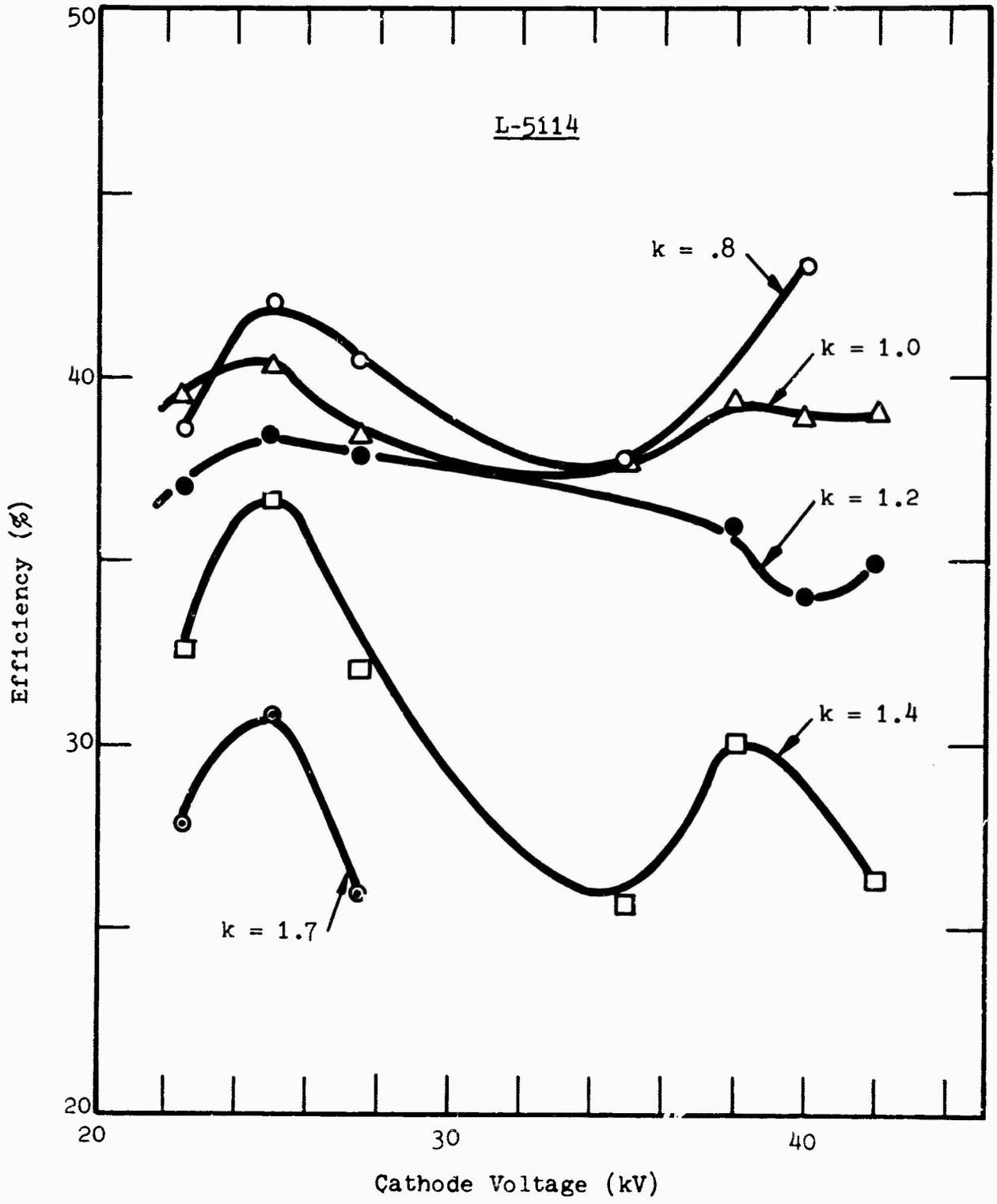

EFFICIENCY VERSUS CATHODE VOLTAGE FOR
DIFFERENT PERVEANCE VALUES

Fig. 15

beam transmission (see Fig. 9), plus the normal reduction in efficiency resulting from higher perveance.

The variation in efficiency with beam voltage may be explained by reference to Mihran's[1] paper. It appears that high voltage, high perveance ESFK designs which result in short drift distances, because of lens design requirements, will probably not provide as high efficiency as at first expected.

1.7 BEAM TESTER

As mentioned in the previous section, the gun used in the tube did not have the correct design dimensions. At this point, it was decided to build a beam tester to compare the results with those obtained from the computer and tube tests.

A cross-sectional view and a photograph of the beam tester can be seen in Figs. 16 and 17. The beam tester essentially consisted of a gun, with the dimensions used in the tube, and a modulating anode operated at ground potential. A carbon target, made from cigarette paper, was located behind the anode and was movable around the expected beam minimum position. In the beam tester, this fragile target was held together by two moly grids. Carbonizing the cigarette paper was quite a problem, because the paper shrinkage was about 30 percent. The carbonizing was done in a vacuum furnace at about 600°C, and the paper was held between two graphite blocks to keep it from wrinkling.

Before welding the glass window assembly to the beam tester body, the target was calibrated with a telescope to

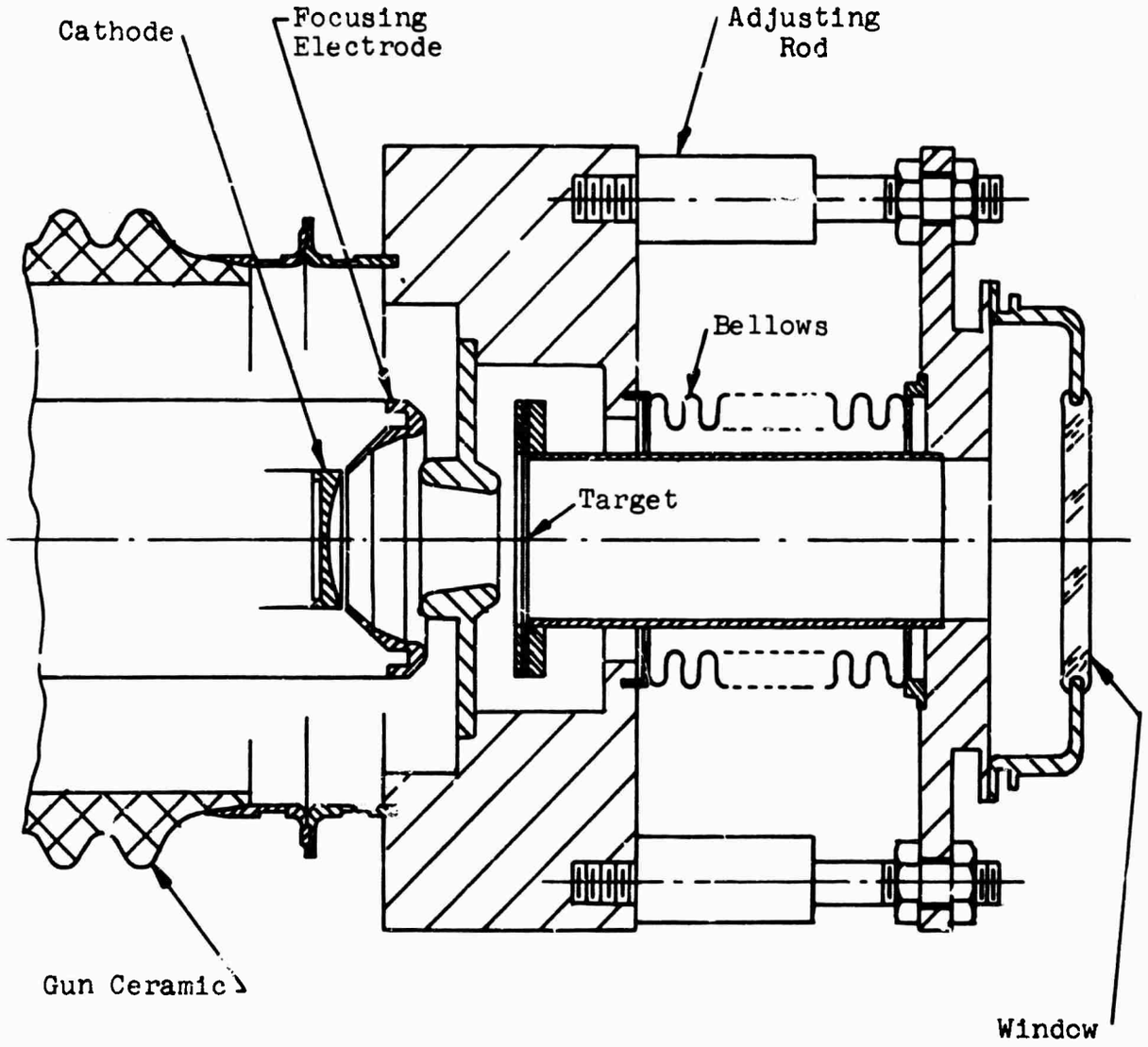

CROSS-SECTIONAL VIEW OF BEAM TESTER

Fig. 16

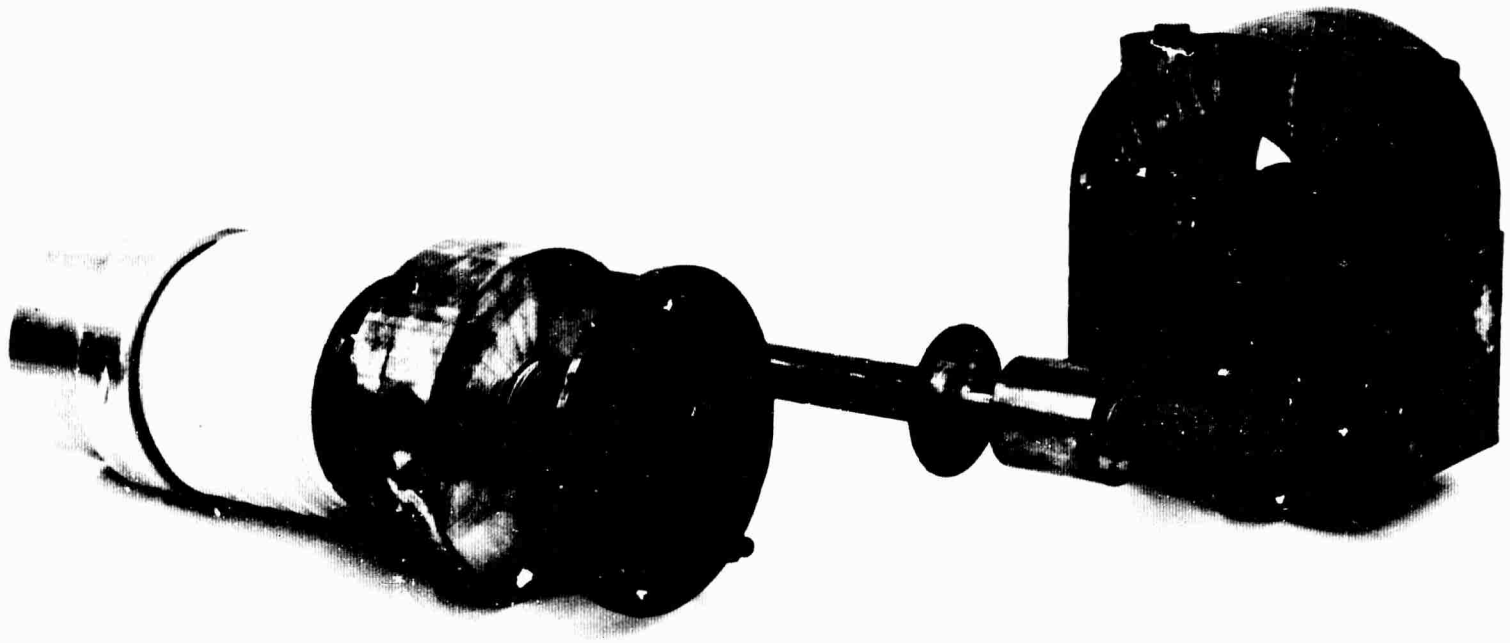

PHOTOGRAPH OF BEAM TESTER

Fig. 17

eliminate any optical errors. Because a lot of outgassing was expected due to beam bombardment of the target, a 5 ℓ/sec appendage vacion pump was welded to the beam tester.

The beam tester was exhausted and processed like a regular tube, but the bakeout temperature was kept around 400°C.

The gun was pulse tested up to 20 kV, but the average beam power was only 5 to 10 watts. At these power levels the target was nicely illuminated and it was possible to measure the beam diameters within .005".

Because the X-ray radiation level started to be dangerous at voltages over 20 kV, it was decided not to go higher in voltage. Another reason that made it unnecessary to go higher was the very close agreement of the results obtained between voltages of 12 and 20 kV.

Surprisingly, as one can see from the following table, the results obtained were very close to those expected from the computer.

	Network and Computer	Beam Tester	Tube
Perveance x 10^{-6} $A/V^{3/2}$	1.74	1.70	1.73
Beam diameter at minimum	.400"	.404"	-
Beam minimum position	0	+.100	

It appears that the beam minimum position in the beam tester may have shifted away from the computer predicted position; however the beam profile (see Fig. 2) was very

flat in that region and it was difficult to measure. Since very good agreement between computed and measured data for this incorrect gun was established, it was decided to rebuild the tube with the correct gun and hopefully get better tube performance.

1.8 EXPERIMENTAL RESULTS OF REBUILT TUBE

As mentioned above, the tube was rebuilt but, again, the obtained results did not show any improvement. This time the space charge limited perveance was 1.39×10^{-6} $A/V^{3/2}$, which indicated that the cathode may have been partly inactive. DC transmission test results, as well as rf test results, were very much comparable to the ones obtained before rebuilding. In conclusion, the tube performance was not improved at all by placing the gun in the proper position.

1.9 GENERAL THEORETICAL STUDIES ON ESFK

1.9.1 Evaluation of a Triple-Gap Extended Interaction Output Cavity in C-Band

The eventual goal of this program was to study the feasibility of a high power, broadband, C-band ESFK. Therefore, some theoretical work has been done on focusing a 2.5 MW beam through a C-band triple-gap extended interaction output cavity. In this study we used the Litton Resistance Network Analogue in combination with a high speed digital computer. The following design objectives were assumed:

Frequency	5500 MHz
RF output power	1 MW
P_{beam}	2.5 MW
Efficiency	40%
Perveance	2×10^{-6} A/$V^{3/2}$
Drift angle $\gamma\ell$	$.7\pi$
Transit angle γd	.7

With these assumed values, the following data could be calculated:

V_{beam}	69 kV
I_{beam}	36.2 Amps
$\gamma_{relativistic}$	2.42 cm^{-1}
ℓ	.91 cm
d	.29 cm

As can be seen, the length of this triple-gap sectic is rather long for focusing a high perveance beam through. Since it was undesirable to use focusing lenses within the triple-gap output cavity, it became necessary to taper the drift tube corresponding to the beam spread curve. Also, a focusing lens was then placed between cavity and collector, as can be seen in Fig. 18.

Several runs were made and are described in the following section.

Figure 19 shows the beam trajectories under dc conditions and compares the cases where the lens was at body potential (ground) and at +10 kV above ground. It is obvious that the lens does not have much focusing effect.

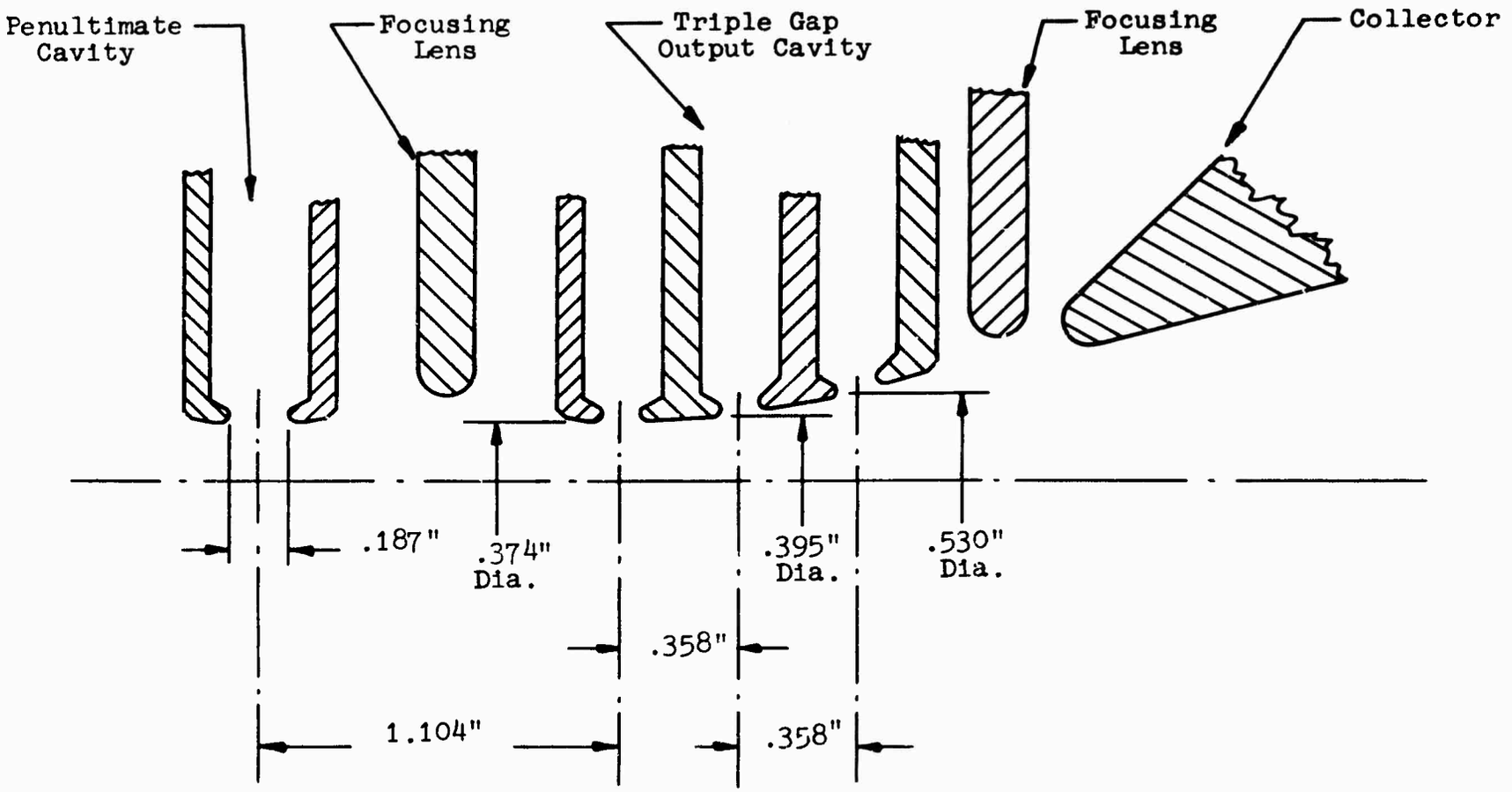

SKETCH OF TRIPLE GAP EXTENDED INTERACTION
C-BAND OUTPUT CAVITY

Fig. 18

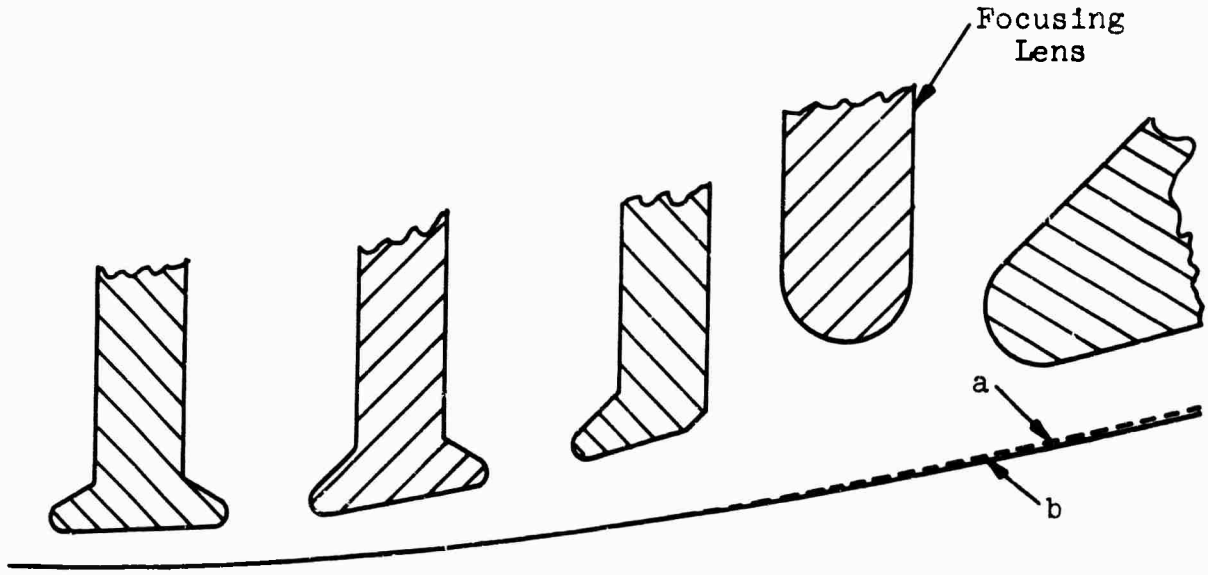

a - Lens at Body Potential (Ground)

b - Lens at +10 kV

ELECTRON TRAJECTORIES UNDER DC CONDITION
FOR TRIPLE GAP OUTPUT CAVITY

Fig. 19

The next figure, No. 20, shows the same cavity configuration, but the beam trajectories are under rf conditions. For these cases, a beam perveance twice as high as that under dc conditions was assumed. Here three different cases are shown. First the lens is at body (ground) potential, second the lens is at +10 kV, and third the lens is at -20 kV with regard to body voltage. Again, the lens does not have much effect and could be eliminated. If the collector nozzle were redesigned by opening up its diameter and by bringing it closer to the cavity, it appears possible to collect the beam completely in the collector.

1.9.2 Beam Power and Perveance Limits for ESFK's

Many times the question arises as to what maximum peak beam power one can expect from an ESFK. Certainly this is dependent upon the frequency and the perveance. It was found worthwhile to study these questions in order to get a rough idea what the limits are. These studies are described in Appendix I.

1.9.3 Calculation of ESFK Small-Signal Gain

Electrostatically focused klystrons consistently exhibit small-signal gains which are significantly in excess of calculated values. Conventional kinematic and space-charge wave theories of klystron bunching are based on the assumption of a constant average velocity of the electrons. In the ESFK this assumption is certainly violated. The introduction of an electrostatic lens into the drift space between cavities alters the rf bunching process since the drift space is no longer field-free.

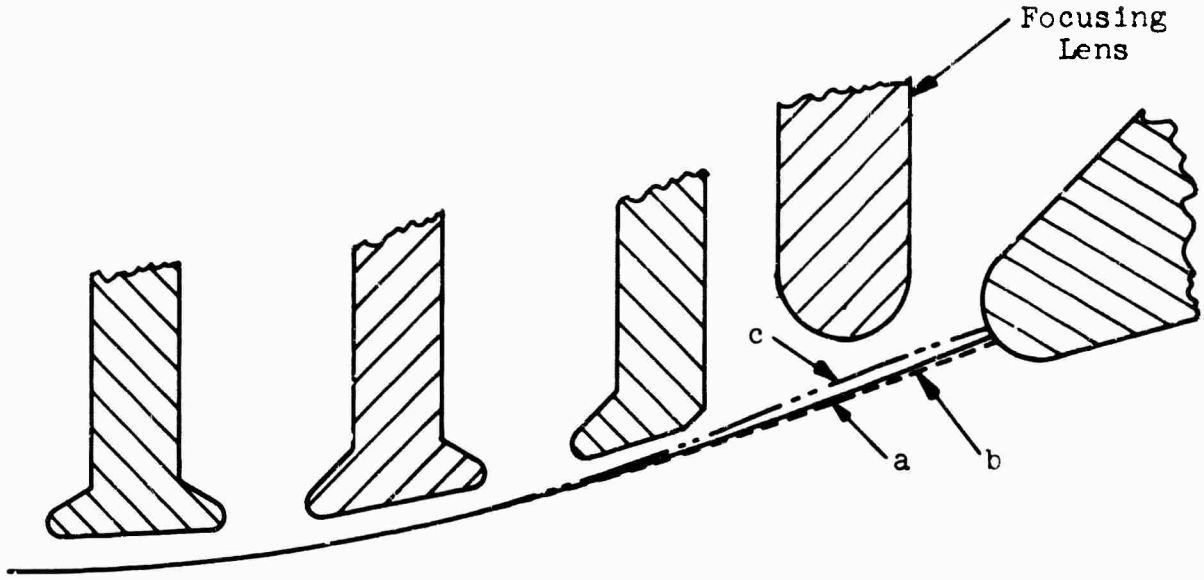

a - Lens at Body Potential (Ground)
b - Lens at +10 kV
c - Lens at -20 kV

ELECTRON TRAJECTORIES UNDER RF CONDITIONS
FOR TRIPLE GAP OUTPUT CAVITY

Fig. 20

In order to adequately predict the small-signal gain of an ESFK a space-charge wave analysis, which accounts for the potential minimum produced by the focusing lens in the drift space, has been made. Details of the analysis are presented in Appendix II.

Simple space-charge wave theory for a field-free drift tube yields the following relationship for the current at the exit plane, $\hat{i}_2$:

$$\hat{i}_2 = -j \frac{\omega}{\omega_q} \rho_o \hat{v}_1 \sin\left(\frac{\omega_q \ell}{\mu_o}\right)$$

where: ω = rf frequency

ω_q = reduced plasma frequency

ρ_o = dc charge density

$\hat{v}_1$ = ac electron velocity at the entrance plane

ℓ = drift distance

μ_o = dc beam velocity

This expression may be written in terms of parameters defined in Appendix II as:

$$\hat{i}_2 = -j \left(\frac{\mu_m}{\mu_o}\right)^{3/2} \frac{\hat{V}_1}{Z_o} \sin\left(\frac{\omega_q \ell}{\mu_o}\right)$$

The dc beam velocity μ_o has been substituted for the dc velocity at the entrance plane of the lens, μ_1, since they are identical.

The maximum value of $\hat{i}_2$ is obtained at the optimum value of drift distance which causes the sin term to be unity. Therefore:

$$\hat{i}'_{2_{opt.}} = -j \left(\frac{\mu_m}{\mu_o}\right)^{3/2} \frac{V_1}{Z_o}$$

This optimum value of rf current at the exit plane is now compared to that of a drift tube of the same length containing an electrostatic lens. Using equation (18) of Appendix II and assuming zero ac current modulation due to the input rf gap ($\hat{i}_1 = 0$, $\hat{V}_1 = \hat{V}_1$), the following relation is obtained:

$$\frac{\hat{i}_2}{\hat{i}'_{2_{opt.}}} = \frac{-j \frac{2\sqrt{2}}{Z_o}\left(\frac{\mu_m}{\mu_o}\right)^2 \left(\frac{\mu_o}{\mu_m} - 1\right)^{1/2}}{-j \left(\frac{\mu_m}{\mu_o}\right)^{3/2} \left(\frac{1}{Z_o}\right)} = 2\sqrt{2} \left(1 - \frac{\mu_m}{\mu_o}\right)^{1/2}$$

Electron velocity is directly proportional to the applied potential, thus:

$$\frac{\mu_m}{\mu_o} = \frac{\sqrt{V_m}}{\sqrt{V_o}} = \sqrt{\Phi_m}$$

$$\frac{\hat{i}_2}{\hat{i}'_{2_{opt.}}} = 2\sqrt{2} \left(1 - \Phi_m{}^{1/2}\right)^{1/2}$$

where ϕ_m is the normalized value of the minimum potential in the lens and is given by the solution of Poisson's equation for a cylindrical beam between lens entrance and exit planes,[2,3,4] as:

$$.0341\ k \left(\frac{L}{b_{ave}}\right)^2 = 1 + 3\phi_m^{1/2} - 4\phi_m^{3/2}$$

where: k = beam microperveance

L = lens period

b_{ave} = average beam radius

Since the lens field cannot penetrate the drift tube much over one tunnel diameter, the maximum value of L used in calculating ϕ_m must be restricted. The following constraints have been placed on L as a result of studies made on several electrostatically focused klystrons:

$$L = L \qquad \text{for } L \leq 5.8\ a$$

$$L = 5.3\ a \qquad \text{for } L > 5.8\ a$$

where a is the drift tube radius.

The small signal transconductance expression for an FSFK may be written as:

$$g_{n,n-1} = \frac{\sqrt{2}\ G_o\ M^2 \left|1 - \phi_m^{1/2}\right|^{1/2}}{\omega_q/\omega} \sin\left(\frac{\omega_q \ell}{u_o}\right)$$

Figure 21 may be used to solve for ϕ_m for a particular beam microperveance and lens geometry. Figure 22 relates $\sqrt{2}\left|1 - \phi_m^{1/2}\right|^{1/2}$ to ϕ_m for convenience in solving the transconductance equation.

In summary, the small-signal gain of an ESFK will be different from that of a conventional klystron because the drift tube is not dc field-free and the rf bunching process is altered. Higher microperveance beams lead to lower values of ϕ_m which result in higher values of gain per stage. The improved accuracy in small-signal gain calculations when the lens correction is made may be seen in the following table.

SUMMARY OF SMALL-SIGNAL GAIN CALCULATIONS

Tube Type	Calculated Values		Measured
	No Lens Correction (dB)	With Lens Cor. (dB)	(dB)
L-5114	45.4	57.6	59.0
L-5044	36.8	48.8	47.2
L-5101	49.6	56.5	58.8
L-3977	49.9	65.9	59.6

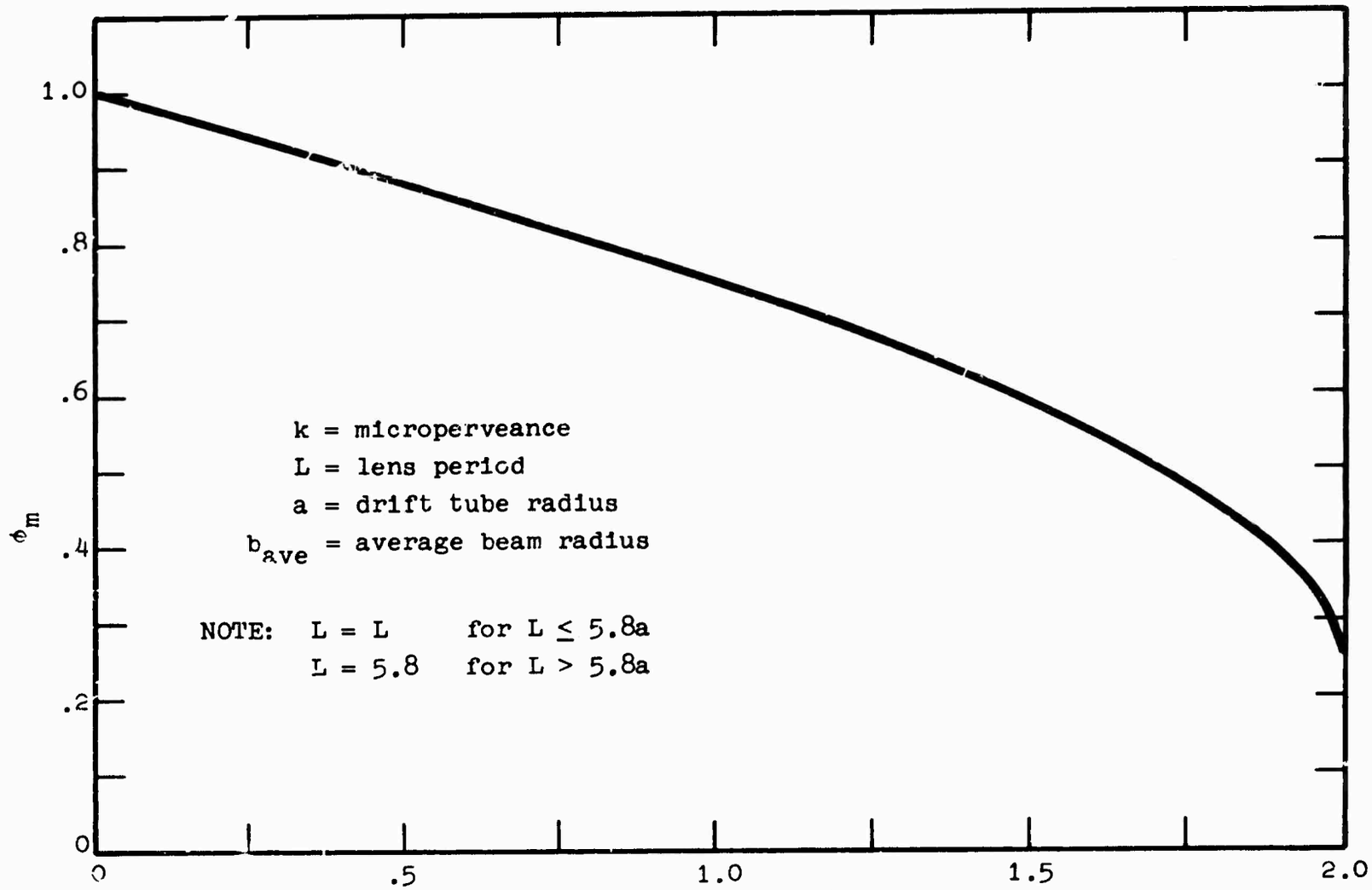

PLOT OF ϕ_m VERSUS $.0341\ k \left(\frac{L}{b_{ave}}\right)^2$

Fig. 21

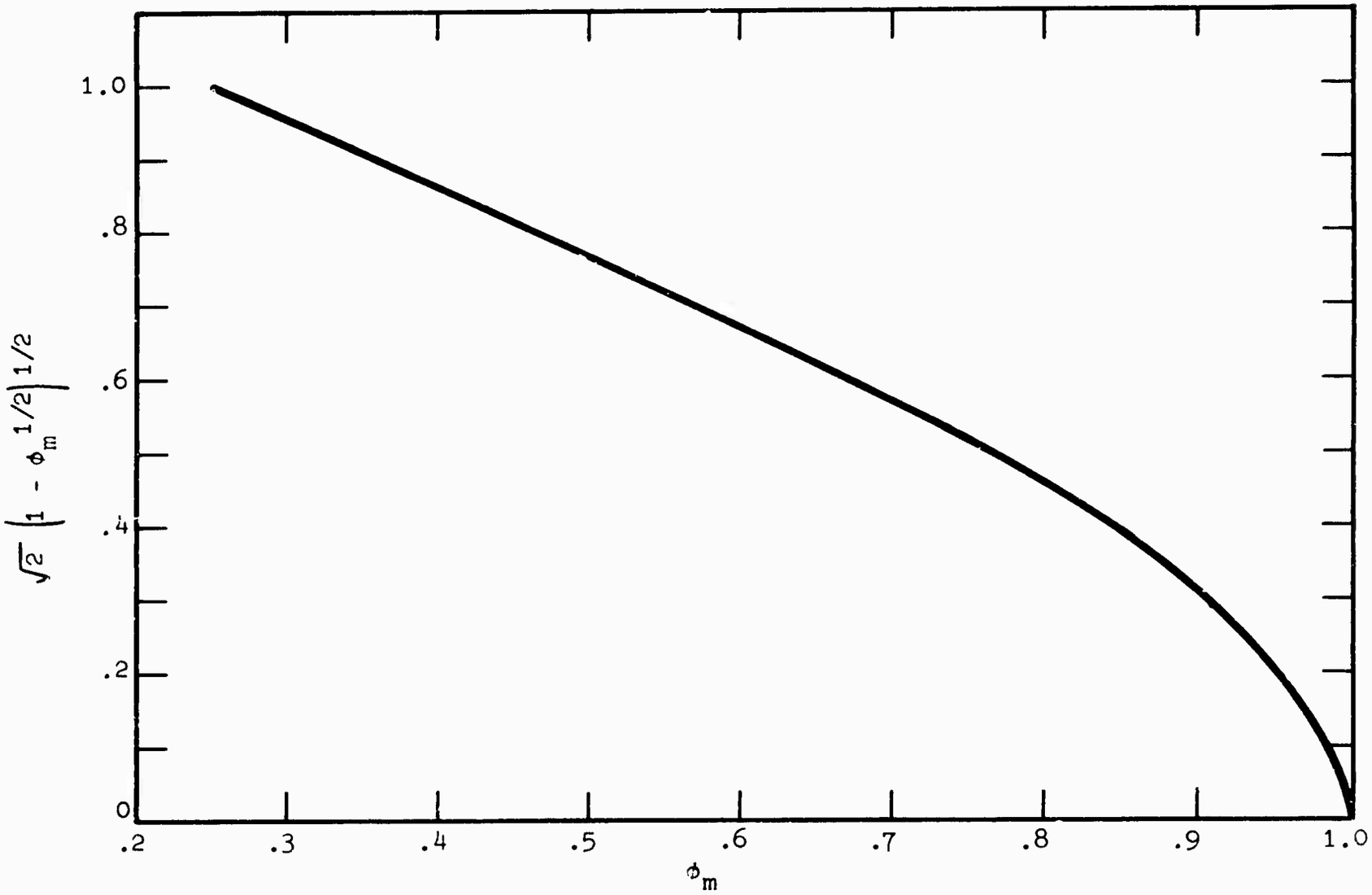

PLOT OF $\sqrt{2}\left(1 - \phi_m^{1/2}\right)^{1/2}$ VERSUS ϕ_m

Fig. 22

2.0 CONCLUSIONS AND RECOMMENDATIONS

This program has demonstrated that high perveance electron beams can be focused by electrostatic lenses. These beams can be successfully utilized in high-power electrostatically focused klystrons. High perveance electron beams present some difficulties because they are not stiffly focused under large-signal rf debunching. This study program has resulted in valuable new knowledge concerning the advantages and limitations of high perveance ESFK's.

The experimental tube constructed during this program performed quite well at voltages lower than the 40 kV design voltage. For instance, at a cathode voltage of 25 kV, for which γa is 1.41, the tube performed as expected. At a perveance of 1.5×10^{-6} $A/V^{3/2}$ the efficiency was 36 percent and at a perveance of 1.72×10^{-6} $A/V^{3/2}$, the efficiency was still 31 percent. For klystron applications where broad bandwidth is badly needed, a high perveance ESFK could provide the solution, possibly with some reduced efficiency. It should be possible to improve the high perveance ESFK performance further by applying all of the new knowledge gained during this program and on other recent ESFK programs. On several new tubes we were able to improve the beam transmission under full rf drive by 30 percent and more. This was possible by redesigning the focusing lens system to compensate for beam spread due to rf debunching. These techniques were unfortunately not known when this program was started.

As the next step it is therefore recommended to build another tube in S- or C-band which incorporates these improvements. We believe that a tube with a perveance of 1.75×10^{-6} $A/V^{3/2}$ could be successfully built. Since an earlier

program definitely demonstrated the feasibility of multiple gap and multiple resonant output filters in broadband output circuit designs, it is felt that a combination of these circuits with a 1.75×10^{-6} $A/V^{3/2}$ perveance beam would lead to an ESFK with up to 8 percent bandwidth at moderate efficiency.

REFERENCES

1. T. Mihran, "The Effect of Drift Length, Beam Radius and Perveance on Klystron Power Conversion Efficiency", IRE Trans. on Electron Devices, April 1967.

2. Fay, Samuel and Shockley, "On the Theory of Space Charge Between Parallel Plane Electrodes", B.S.T.J., January 1938.

3. Spangenberg, Vacuum Tubes, McGraw-Hill, 1948, pp. 248-259.

4. A. Sutherland, "Relaxation Instabilities in High-Perveance Electron Beams", IRE Trans. on Electron Devices, October 1960, pp. 268-273.

5. J.R. Pierce, "Theory and Design of Electron Beams", D. Van Nostrand, 1954, pp. 194-207.

6. A. Beck, Space Charge Waves, Pergamon Press, 1958, pp. 136-138.

7. H.G. Kosmahl, "Propagation of Space-Charge Waves in Diodes and Drift Spaces", IRE Trans. on Electron Devices, April 1959, p. 225.

APPENDIX I

BEAM POWER AND PERVEANCE LIMITS FOR ELECTROSTATICALLY FOCUSED KLYSTRONS

BLANK PAGE

APPENDIX I

BEAM POWER AND PERVEANCE LIMITS FOR ELECTROSTATICALLY FOCUSED KLYSTRONS

A fundamental requirement for periodic electron beam focusing systems is that there exists a maximum permissible axial spacing between lenses, which cannot be exceeded without resulting in beam blow-up. An excellent insight into this requirement has been given by Pierce.[5] He considers a sequence of thin electron lenses, separated by an axial spacing L, through which an electron beam flows. (Pierce's Fig. 11.6). In the plane of the lens the electron beam has a radius r_o and, in that plane, each electron receives a radial impulse toward the axis of symmetry due to the action of the lens field. Between lenses, the only dc forces acting on the beam are those due to its own space-charge, which causes it to spread.

Pierce's Fig. 9.2 shows the beam spread action as predicted by the "universal beam spread" equation. This figure illustrates the fact that there exists a maximum axial distance beyond which the beam cannot travel without exceeding its original radius. If the radius is not to be allowed to grow larger, then another lens must be placed at this maximum distance. Pierce's Fig. 11.8 shows the initial negative slope required to cause an electron beam to return to its original radius as a function of distance between lenses. The maximum distance expressed in normalized units is 2.16. This may be stated as:

$$\left(\frac{.174\sqrt{k}}{r_o}\right) L \leq 2.16$$

where: k = beam microperveance

r_o = beam radius at lens

L = spacing between lenses

This expression is valid provided the lenses are thin and have no spherical aberrations. This is not true in practice. In addition, when a density-modulated electron beam must be focused by such a lens system, the effective microperveance may be up to twice the value for a dc beam. The expression for the maximum lens spacing for an electrostatically focused klystron will be assumed to be:

$$\left(\frac{.174\sqrt{k}}{r_o}\right) L = 1.5$$

It is now instructive to express the maximum lens spacing in terms of klystron design parameters. The beam radius r_o at the lens plane can be expressed in terms of the normalized klystron gap radius γa and the electron wave number. (Relativistic effects are ignored).

$$r_o = \left(\frac{r_o}{a}\right) (\gamma a) \left(\frac{1}{\gamma}\right)$$

where: a = gap radius

$$\gamma = \frac{\omega}{\mu_o} = \left(\frac{2\pi}{\lambda}\right) \left(\frac{506}{V_o^{\frac{1}{2}}}\right)$$

V_o = dc beam voltage

λ = free-space wavelength

The dc beam voltage is related to the dc beam power, W_o and the beam microperveance k as follows:

$$V_o^{\frac{1}{2}} = \left(\frac{10^9 \, W_{o_{kw}}}{k}\right)^{1/5}$$

Substituting for $V_o^{\frac{1}{2}}$:

$$\gamma = \left[\frac{(2\pi)\,(506)\,(10)^{1/5}}{10^2}\right] \frac{k^{1/5}}{\lambda \, W_{o_{kw}}^{\;1/5}} \quad .$$

Substituting for γ:

$$r_o = \left[\frac{10^2}{(2\pi)\,(506)\,(10)^{1/5}}\right] \frac{\lambda \, W_{o_{kw}}^{\;1/5}}{k^{1/5}} \, (\gamma a) \, \left(\frac{r_o}{a}\right) \quad .$$

Substituting for r_o in the maximum lens spacing expression:

$$\left[\frac{(0.174)\,(2\pi)\,(506)\,(10)^{1/5}}{10^2}\right] \frac{k^{1/5}\sqrt{k}}{W_{o_{kw}}^{\;1/5} \, (\gamma a) \, \left(\frac{r_o}{a}\right)} \left(\frac{L}{\lambda}\right) = 1.5$$

For a typical klystron design, the product of $\frac{r_o}{a}$ and γa would be very close to unity. Therefore, by assuming $\left(\frac{r_o}{a}\right)(\gamma a) = 1.0$, the maximum lens spacing relation becomes:

$$\frac{L}{\lambda} = (.171) \, \frac{W_{o_{kw}}^{\;1/5}}{k^{7/10}}$$

Figure 1 is a plot of the maximum permissible axial lens spacing normalized by the free-space wavelength, vs peak beam power, with microperveance as a parameter. It may be observed that the choice of electron beam microperveance has a pronounced effect on the maximum permissible lens spacing.

Having determined the maximum lens spacing as a function of beam power, microperveance, and wavelength, it is now possible to determine the ultimate limits of ESFK design. Figure 2 depicts the cavity-lens configuration of an ESFK. The spacing between lenses must allow for a lens electrode of thickness T, two high voltage gaps of width S, two cavity walls of thickness w, and a cavity resonator of height H. The lens spacing may be expressed as:

$$L = 2\,(S + w) + T + H \quad .$$

The lens-gap spacing depends upon the operating voltage, which will be assumed equal to the beam voltage, and the allowable voltage gradient. For a maximum voltage gradient of 118 kV/cm(300 v./mil.):

$$S = \frac{1}{29.8}\left(\frac{W_{o_{kw}}}{k}\right)^{2/5} \quad .$$

A typical cavity gap transit angle, γd, would be 1.1 radians. For reasonable values of R/Q, the cavity height should not be less than 2 γd. Therefore, the assumption of $H = 2\,\gamma d$ is made, or:

$$H = \frac{2.2\lambda}{50.4}\left(\frac{W_{o_{kw}}}{k}\right)^{1/5} \quad .$$

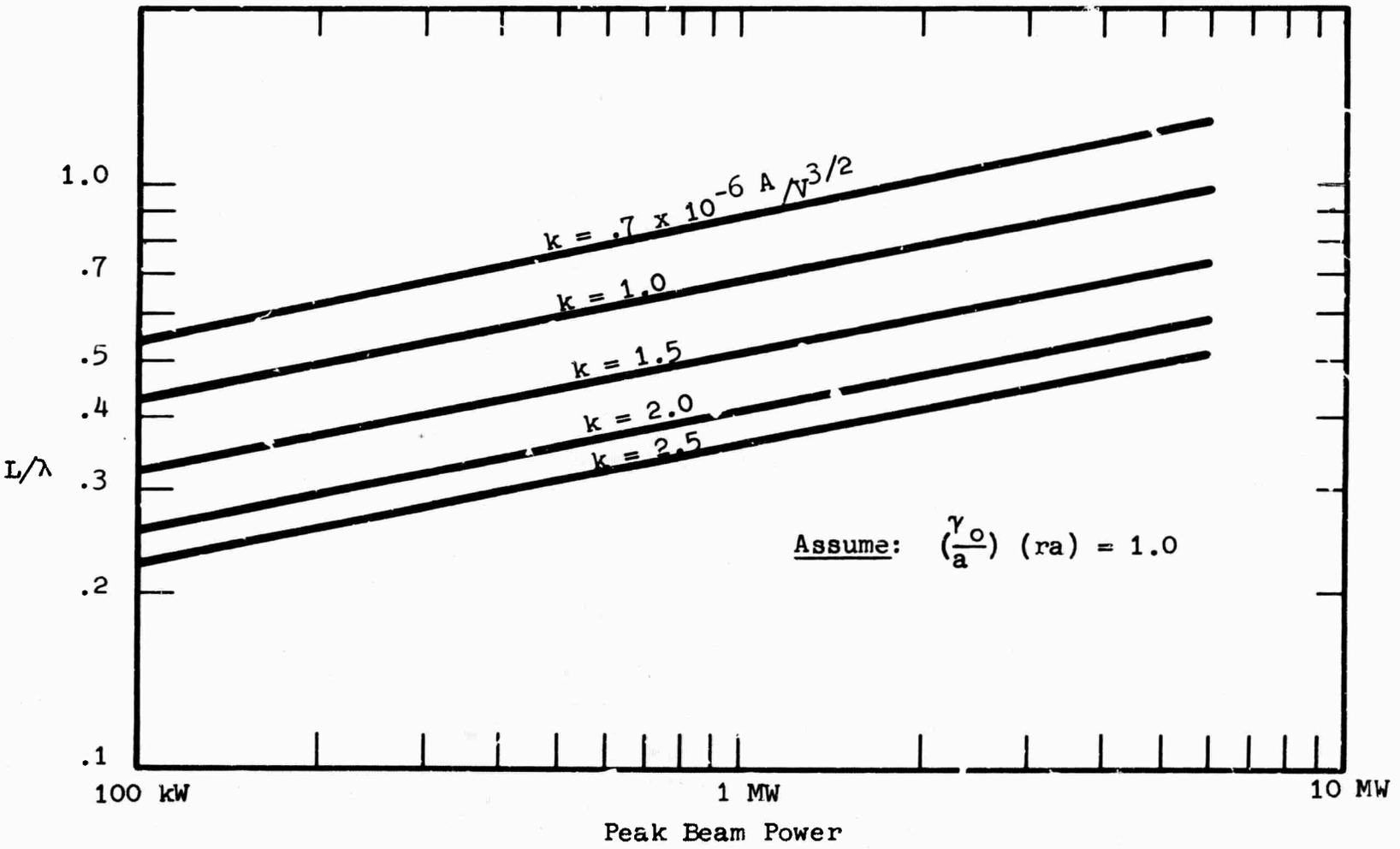

MAXIMUM NORMALIZED LENS SPACING VS
BEAM POWER FOR ELECTROSTATICALLY FOCUSED KLYSTRON

Fig. 1

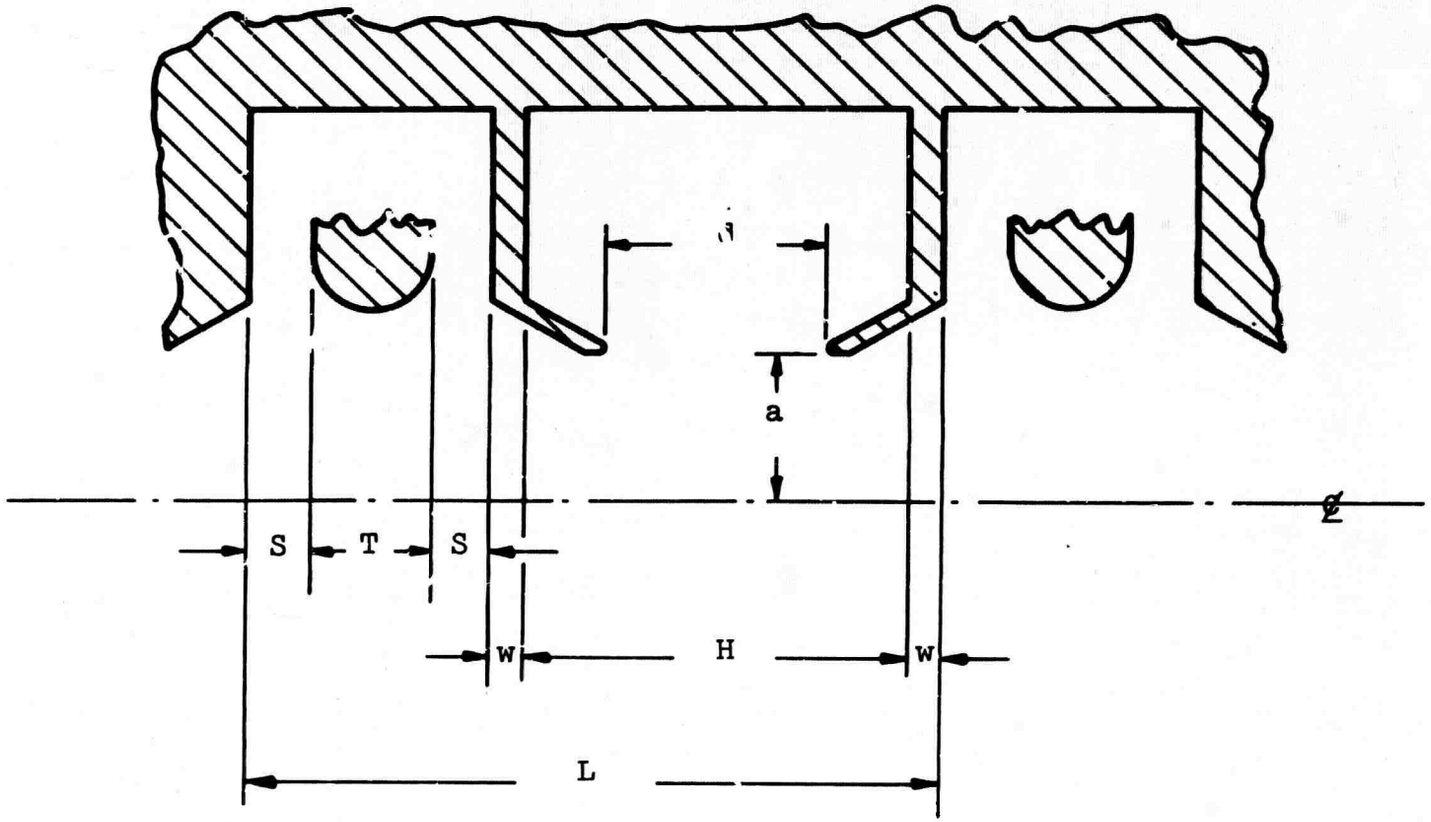

CAVITY-LENS CONFIGURATION

Fig. 2

The lens electrode thickness may be approximated by assuming that its radius of curvature should be no less than S/2 in order to prevent excessive local electric field gradients. Therefore, it is assumed that T = S.

The minimum cavity wall thickness, W, is not easy to specify because it depends on the cavity diameter and the average power of the klystron. The following values will be used in the analysis which follows:

$$w = .03\ \lambda \quad \text{at 10 cm}$$

$$w = .04\ \lambda \quad \text{at 5 cm}$$

$$w = .06\ \lambda \quad \text{at 3 cm.}$$

The minimum lens spacing may now be expressed as:

$$L = 3\ S + 2\ \gamma\ d + 2\ W$$

or

$$L = .1\ \left(\frac{W_{o_{kw}}}{k}\right)^{2/5} + .0436\ \lambda\ \left(\frac{W_{o_{kw}}}{k}\right)^{1/5} + 2\ N\lambda \quad ,$$

where: $N = .03$ at $\lambda = 10$ cm

$N = .04$ at $\lambda = 5$ cm

$N = .06$ at $\lambda = 3$ cm.

Normalizing with respect to free-space wavelength:

$$L/\lambda = \frac{.1}{\lambda}\left(\frac{W_{o_{kw}}}{k}\right)^{2/5} + .0436\left(\frac{W_{o_{kw}}}{k}\right)^{1/5} + 2N \quad .$$

This expression was solved for various values of peak beam power and microperveance at wavelengths of 10 cm, 5 cm, and 3 cm. The values of normalized maximum lens spacing are plotted along with the values of minimum lens spacing in Figs. 3 through 6. Where the two curves intersect determines the maximum beam power limit for an ESFK for a given microperveance and wavelength. Similarly, the maximum beam microperveance for an ESFK may be determined for a given peak beam power and wavelength.

An expression for the maximum microperveance and/or maximum peak beam power for an ESFK at a given wavelength may be obtained by equating the expressions for maximum and minimum lens spacings.

$$.171 \frac{\left(\frac{W_{o_{kw}}}{k \cdot 7}\right)^{1/5}}{} \approx \frac{.1}{\lambda} \left(\frac{W_{o_{kw}}}{K}\right)^{2/5} + .0436 \left(\frac{W_{o_{kw}}}{K}\right)^{1/5} + 2N$$

Examination of Fig. 3 indicates the maximum beam microperveance for high power klystrons in S-band to be equal to, or greater than, 2.5. Figure 4 indicates that megawatt klystrons are feasible in C-band with microperveance 1.0 beams. Increasing the microperveance to 1.5 in C-band reduces the feasible klystron power level, as seen in Fig. 5. At X-band, it is no longer possible to construct a high power ESFK with a desirable beam microperveance. Figure 6 indicates a maximum beam power limit of 650 kW for a 0.7 microperveance beam at 3 cm.

The limitation of beam perveance with frequency implies a limitation on the klystron bandwidth since it can be shown that bandwidth is directly proportional to $k^{4/5}$.

This analysis of beam power and perveance limits for the ESFK is, of necessity, based on many assumptions whose

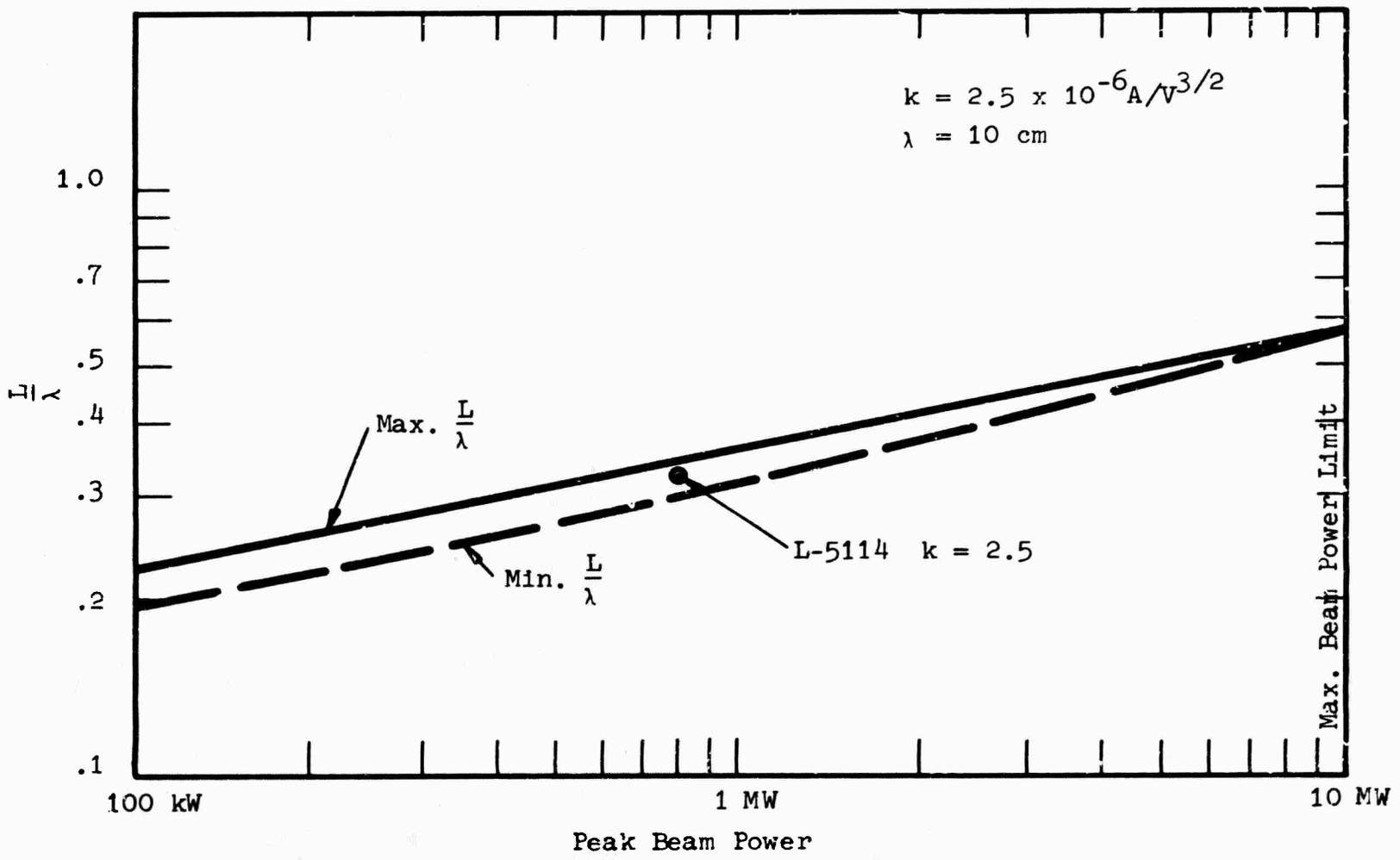

MAXIMUM AND MINIMUM NORMALIZED LENS SPACING
VS BEAM POWER FOR ELECTROSTATICALLY FOCUSED KLYSTRON

Fig. 3

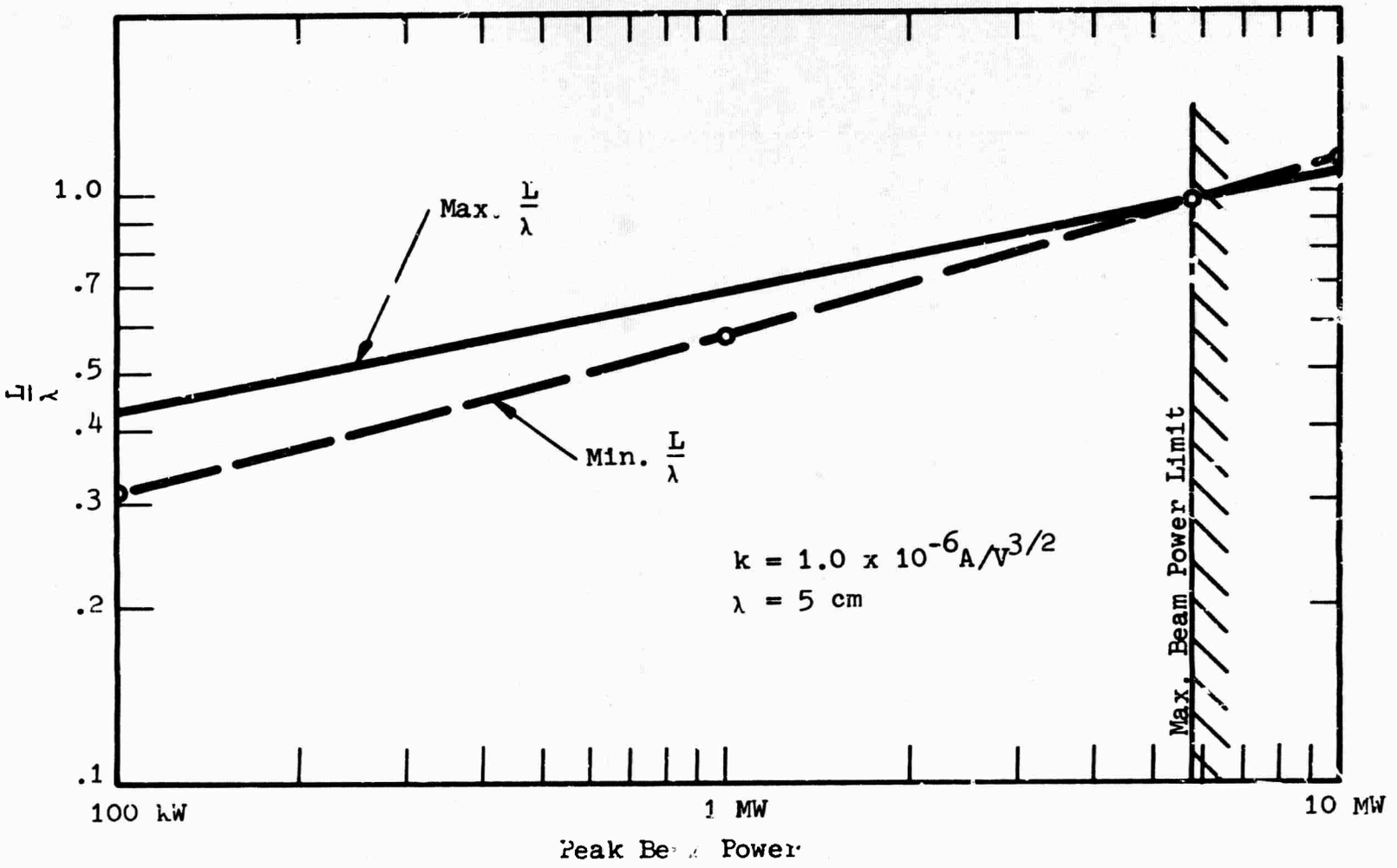

MAXIMUM AND MINIMUM NORMALIZED LENS SPACING
VS BEAM POWER FOR ELECTROSTATICALLY FOCUSED KLYSTRON

Fig. 4

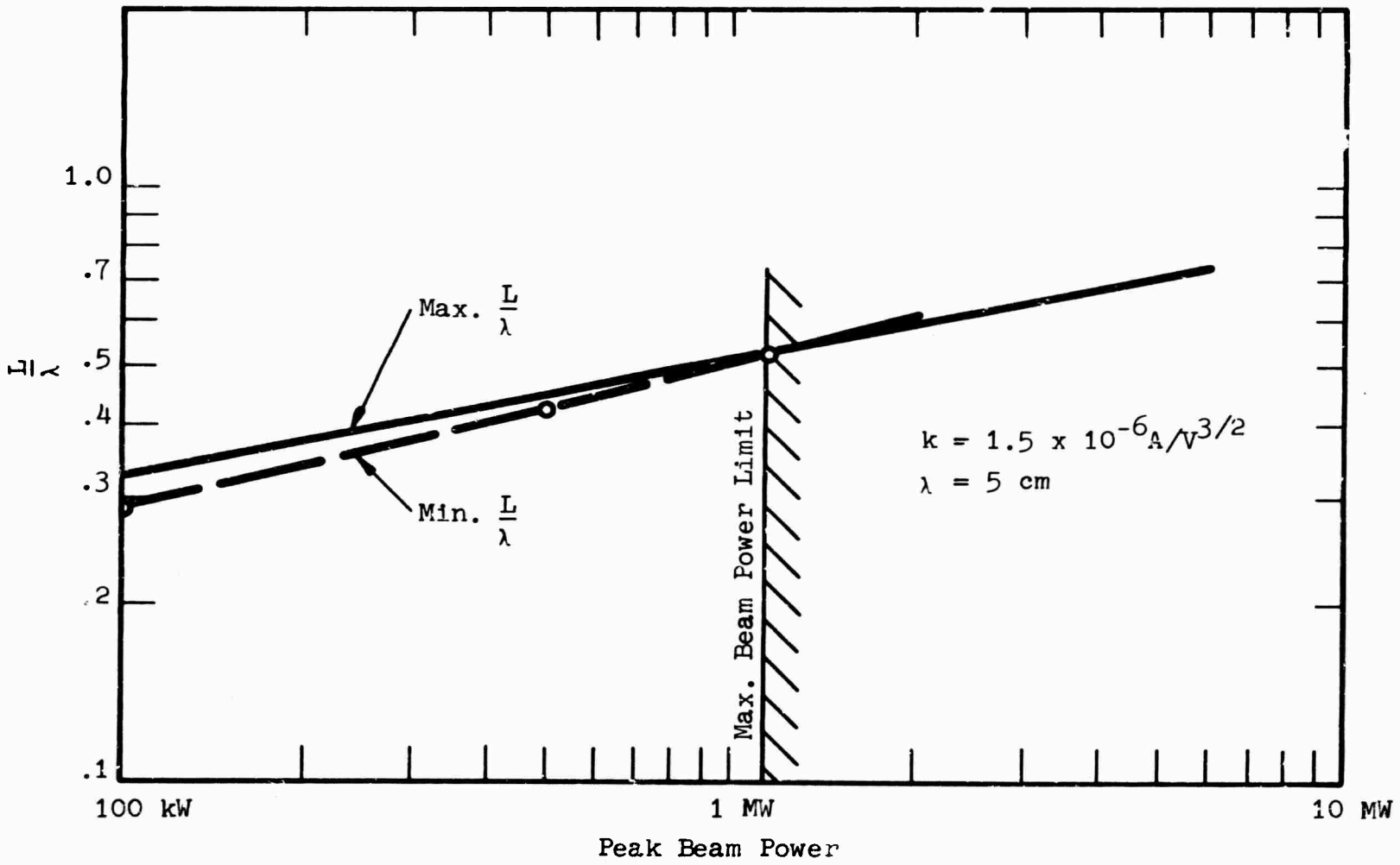

MAXIMUM AND MINIMUM NORMALIZED LENS SPACING
VS BEAM POWER FOR ELECTROSTATICALLY FOCUSED KLYSTRON

Fig. 5

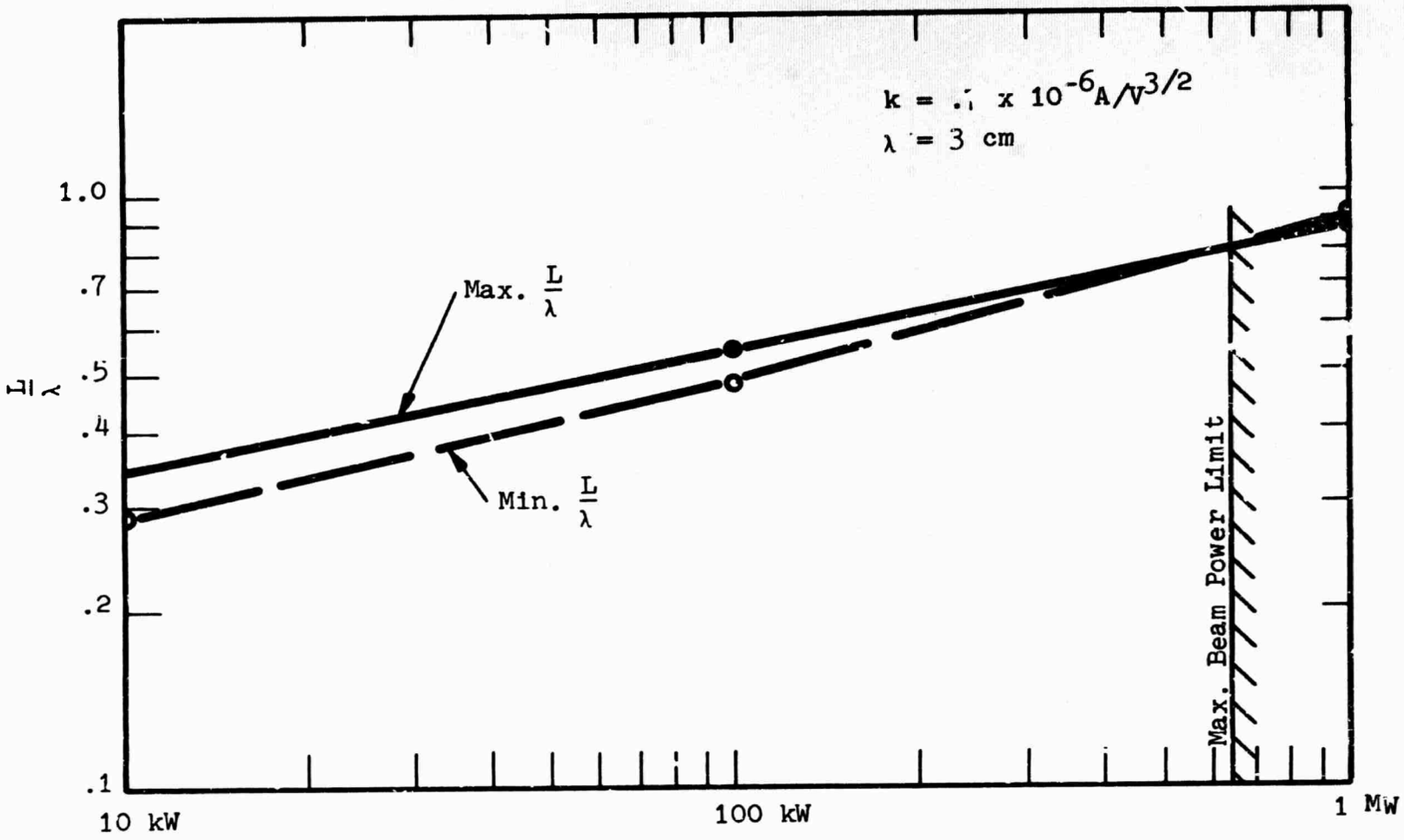

MAXIMUM AND MINIMUM NORMALIZED LENS SPACING
VS BEAM POWER FOR ELECTROSTATICALLY FOCUSED KLYSTRON

Fig. 6

validity is open to question. The assumption of $(r_o/a)(\gamma a) = 1.0$ is very conservative; whereas, the assumption of $T = S$ is not conservative. Practical considerations such as voltage breakdown, body cooling, and cavity conductance requirements will doubtless alter the limits defined herein. However, it is hoped that this analysis will provide a useful "ballpark" estimate of the ultimate limits of the ESFK.

APPENDIX II

SPACE-CHARGE WAVE ANALYSIS OF THE ESFK LENS CELL

APPENDIX II

SPACE-CHARGE WAVE ANALYSIS OF THE ESFK LENS CELL

The following expressions are defined:

$$i[z,t] = -i_o[z] + i_1[z]e^{j\omega t} \qquad \text{convection current density}$$

$$\rho[z,t] = -\rho_o[z] + \rho_1[z]e^{j\omega t} \qquad \text{space-charge density}$$

$$v[z,t] = \mu_o[z] + v_1[z]e^{j\omega t} \qquad \text{electron velocity}$$

By making the transformation of variables:

$$i_1[z] = \hat{i}[z]e^{-j\omega\tau[z]}$$

$$v_1[z] = \hat{v}[z]e^{-j\omega\tau[z]}$$

where: $\tau[z] = \int_o^z \frac{dz}{\mu_o[z]}$

it can be shown that the following differential equations apply for $i(z)$ and $v(z)$. (6)

$$\frac{d^2\hat{i}[z]}{dz^2} + \frac{3}{\mu[z]}\frac{d\mu[z]}{dz}\frac{d\hat{i}[z]}{dz} + \frac{\eta i_o}{\epsilon\mu^3[z]}\hat{i}[z] = 0 \qquad (1)$$

$$\hat{v}[z] = j\frac{\mu^2[z]}{\omega i_o}\frac{d\hat{i}[z]}{dz} \qquad (2)$$

where: $\eta = \frac{|e|}{m}$

Using the Llewellyn equations of motion,

$$\frac{d^2v}{dt^2} = - \frac{\eta I}{\epsilon}$$

where: $$I = i + \epsilon \frac{\partial E}{\partial t}$$

the dc component can be separated out to obtain a differential equation relating dc velocity to the dc beam current density, thereby taking complete account of the dc space charge effects.

$$\frac{d^2\mu}{dt^2} = \frac{\eta}{\epsilon} i_o \tag{3}$$

This expression can be integrated twice with respect to time to obtain an expression for μ as a function of the transit time of an electron. The instant at which the electron crosses the plane of the potential minimum in the lens (e.g. its center) will be $t = 0$. Thus, by definition, at $t = 0$ the acceleration is zero.

$$\frac{d\mu}{dt} = \frac{\eta i_o}{\epsilon} t \tag{4}$$

$$\mu = \frac{\eta i_o}{\epsilon} \frac{t^2}{2} + \mu_m \tag{5}$$

$$z = \frac{\eta i_o}{\epsilon} \frac{t^3}{6} + \mu_m t + z_m \tag{6}$$

where μ_m and z_m are the velocity and position, respectively, of the pctential minimum.

Following Kosmahl[7], and transforming the independent variables in equations (1) and (2) from z to μ, will require an expression for $d\mu/dz$. This is obtained from (4) and (5).

$$\frac{d\mu}{dz} = \frac{d\mu/dt}{dz/dt} = \frac{d\mu/dt}{\mu} = \frac{\eta i_o}{\epsilon}\frac{t}{\mu} = K\frac{t}{\mu} \tag{7}$$

Solving (5) for t, and substituting into (7) eliminates t.

$$\frac{d\mu}{dz} = \frac{\pm\sqrt{2K(\mu - \mu_o)}}{\mu} \tag{8}$$

where: $K = \dfrac{\eta i_o}{\epsilon}$ (9)

The + sign in (8) applies to the right of the potential minimum, and the - sign applies to the left.

Equations (1) and (2) are now transformed to:

$$\mu(\mu - \mu_m)\frac{d^2\hat{i}}{d\mu^2} + (5/2\mu - 2\mu_m)\frac{d\hat{i}}{d\mu} + \frac{\hat{i}}{2} = 0 \tag{10}$$

$$\hat{v} = \pm j\frac{\mu^2}{\omega i_o}\sqrt{\frac{2K(\mu - \mu_m)}{\mu^2}}\frac{d\hat{i}}{d\mu} \tag{11}$$

These equations have solutions of the form:

$$\hat{i} = A\mu^{-1}(\mu - \mu_m)^{1/2} + B\mu^{-1} \tag{12}$$

$$\hat{v} = \pm j\frac{\sqrt{2K}}{\omega i_o \mu}\left[A(\mu - \frac{\mu_m}{2}) - B(\mu - \mu_m)^{1/2}\right] \tag{13}$$

The arbitrary constants A and B must be chosen to match the boundary conditions. Let the ac current and ac velocity at the entrance plane of the lens cell be $\hat{i}_1$ and $\hat{v}_1$, respectively. At the same plane, the dc velocity is μ_1. Substituting these conditions into (12) and (13) and taking cognizance of the fact that the entrance plane of the lens cell is to the left of the potential minimum, the following results are obtained.

To the left of the potential minimum:

$$\hat{V} = \hat{V}_1 \left(\frac{\mu_m}{\mu_1}\right)\left[\left(2 - \frac{\mu}{\mu_m}\right) + 2\left(\frac{\mu}{\mu_m} - 1\right)^{1/2}\left(\frac{\mu_1}{\mu_m} - 1\right)^{1/2}\right]$$

$$+ j\sqrt{2}\, Z_o \hat{i}_1 \left[\left(\frac{\mu}{\mu_m} - 1\right)^{1/2}\left(2 - \frac{\mu_1}{\mu_m}\right) - \left(\frac{\mu_1}{\mu_m} - 1\right)^{1/2}\left(2 - \frac{\mu}{\mu_m}\right)\right] \qquad (14)$$

$$\hat{i} = j\,\frac{\sqrt{2}\hat{V}_1}{Z_o}\left(\frac{\mu_m}{\mu}\right)\left(\frac{\mu_m}{\mu_1}\right)\left[\left(\frac{\mu}{\mu_m} - 1\right)^{1/2} - \left(\frac{\mu_1}{\mu_m} - 1\right)^{1/2}\right]$$

$$+ \hat{i}_1\left(\frac{\mu_m}{\mu}\right)\left[\left(2 - \frac{\mu_1}{\mu_m}\right) + 2\left(\frac{\mu_1}{\mu_m} - 1\right)\left(\frac{\mu}{\mu_m} - 1\right)^{1/2}\right] \qquad (15)$$

To the right of the potential minimum:

$$\hat{V} = \hat{V}_1\left(\frac{\mu_m}{\mu_1}\right)\left[\left(2 - \frac{\mu}{\mu_m}\right) - 2\left(\frac{\mu}{\mu_m} - 1\right)^{1/2}\left(\frac{\mu_1}{\mu_m} - 1\right)^{1/2}\right]$$

$$- j\sqrt{2}\, Z_o \hat{i}_1\left[\left(\frac{\mu}{\mu_m} - 1\right)^{1/2}\left(2 - \frac{\mu_1}{\mu_m}\right) + \left(\frac{\mu_1}{\mu_m} - 1\right)^{1/2}\left(2 - \frac{\mu}{\mu_m}\right)\right] \qquad (16)$$

$$\hat{i} = -j\frac{\sqrt{2}\hat{V}_1}{Z_o}\left(\frac{\mu_m}{\mu_1}\right)\left(\frac{\mu_m}{\mu}\right)\left[\left(\frac{\mu}{\mu_m} - 1\right)^{1/2} + \left(\frac{\mu_1}{\mu_m} - 1\right)^{1/2}\right]$$

$$+ \hat{i}_1\left(\frac{\mu_m}{\mu}\right)\left[\left(2 - \frac{\mu_1}{\mu_m}\right) - 2\left(\frac{\mu}{\mu_m} - 1\right)^{1/2}\left(\frac{\mu_1}{\mu_m} - 1\right)^{1/2}\right] \qquad (17)$$

where: $\hat{V} = \frac{\mu \hat{v}}{\eta}$ and $Z_o = \frac{\mu_m^{3/2}}{\omega\epsilon\sqrt{K}}$

Equations (14) through (17) define a general matrix relating the ac current modulation and ac velocity modulation at any plane in the lens cell where the dc velocity is μ to the corresponding quantities at the entrance plane where the known dc velocity is μ_1. The dc velocity μ is a known function of z through the Fay, Samuel, Shockley solutions to Poisson's equation.(2)

What is of primary interest is not the ac velocity and current within the lens cell but the value of these quantities at the exit plane. The dc velocity at the exit plane will be equal to the dc beam velocity at the entrance plane. By setting $\mu = \mu_1$ in (16) and (17), the following matrix relation between the ac quantities at the exit plane and the entrance plane is obtained:

$$\begin{bmatrix} \hat{V}_2 \\ \hat{i}_2 \end{bmatrix} = \begin{bmatrix} (4\frac{\mu_m}{\mu_1} - 3) & -2j\sqrt{2}\, Z_o(2-\frac{\mu_1}{\mu_m})(\frac{\mu_1}{\mu_m} - 1)^{1/2} \\ -j\frac{2\sqrt{2}}{Z_o}(\frac{\mu_m}{\mu_1})^2(\frac{\mu_1}{\mu_m} - 1)^{1/2} & (4\frac{\mu_m}{\mu_1} - 3) \end{bmatrix} \cdot \begin{bmatrix} \hat{V}_1 \\ \hat{i}_1 \end{bmatrix} \qquad (18)$$

Security Classification

DOCUMENT CONTROL DATA - R & D

(Security classification of title, body of abstract and indexing annotation must be entered when the overall report is classified)

1. ORIGINATING ACTIVITY (Corporate author)
Litton Precision Products, Inc.
dba Litton Industries, Electron Tube Division
960 Industrial Rd, San Carlos, Calif. 94070

2a. REPORT SECURITY CLASSIFICATION
Unclassified

2b. GROUP

3. REPORT TITLE

STUDY OF HIGH-POWER ELECTROSTATICALLY FOCUSED KLYSTRONS

4. DESCRIPTIVE NOTES (Type of report and inclusive dates)
Final Report, 1 May 66 to 28 Aug 67

5. AUTHOR(S) (First name, middle initial, last name)

T. H. Luchsinger and W. R. Day

6. REPORT DATE	7a. TOTAL NO. OF PAGES	7b. NO. OF REFS
November 1967	41, Appendix I - 13 Appendix II - 6	7

8a. CONTRACT OR GRANT NO.	9a. ORIGINATOR'S REPORT NUMBER(S)
DA 28-043 AMC-02253(E)	
b. PROJECT NO. 7910-21-223-04-00-50	
c.	9b. OTHER REPORT NO(S) (Any other numbers that may be assigned this report) ECOM-02253-F
d.	

10. DISTRIBUTION STATEMENT
This document has been approved for public release and sale; its distribution is unlimited.

11. SUPPLEMENTARY NOTES	12. SPONSORING MILITARY ACTIVITY
Sponsored by: Advanced Research Projects Agency, ARPA Order No. 436	U. S. Army Electronics Command Fort Monmouth, New Jersey 07703 Attn: AMSEL-KL-TM

13. ABSTRACT

This report covers a 15-month program of experimental study to establish the feasibility of employing higher perveance beams in ESFK's, which together with other broadband techniques (filter, extended interaction cavity) would lead to ten percent bandwidth. In order to keep the tube design as simple as possible, this program was undertaken only to study the feasibility of employing higher beam perveances in ESFK's.

In addition to the experimental study, further theoretical studies were made on a triple-gap extended interaction cavity leading to a 1 MW peak power C-band klystron with ten percent bandwidth. Studies of beam power and perveance limits for ESFK's were made. An improved method was developed for calculating small-signal gain of ESFK's which accounts for the effect of the electrostatic field of the lens on the electron bunching process.

During this program, one beam tester and one electrostatically focused klystron were built. By utilizing very low perveances ($.8 \times 10^{-6}$ A/V$^{3/2}$) efficiencies of up to 43 percent were achieved. By increasing the perveance to 1.5×10^{-6} A/V$^{3/2}$ the efficiency dropped to 36 percent. Beam perveances higher than approximately 1.75×10^{-6} A/V$^{3/2}$ do not appear useful in ESFK's.

DD FORM 1 NOV 65 1473 REPLACES DD FORM 1473, 1 JAN 64, WHICH IS OBSOLETE FOR ARMY USE.

Security Classification

14. KEY WORDS	LINK A		LINK B		LINK C	
	ROLE	WT	ROLE	WT	ROLE	WT
Electrostatic Focusing Broadband Klystron High Perveance Beams						